

SATELLITE MONITORING OF CURRENT AND HISTORICAL DEVELOPMENT
PATTERNS IN BIG SKY, MONTANA: 1990-2005

by

Natalie Monique Campos

A thesis submitted in partial fulfillment
of the requirements for the degree

of

Master of Science

in

Land Resources and Environmental Sciences

MONTANA STATE UNIVERSITY
Bozeman, Montana

May, 2008

© COPYRIGHT

by

Natalie Monique Campos

2008

All Rights Reserved

APPROVAL

of a thesis submitted by

Natalie Monique Campos

This thesis has been read by each member of the thesis committee and has been found to be satisfactory regarding content, English usage, format, citation, bibliographic style, and consistency, and is ready for submission to the Division of Graduate Education.

Dr. Rick L. Lawrence

Approved for the Department of Land Resources and Environmental Sciences

Dr. Jon M. Wraith

Approved for the Division of Graduate Education

Dr. Carl A. Fox

STATEMENT OF PERMISSION TO USE

In presenting this thesis in partial fulfillment of the requirements for a master's degree at Montana State University, I agree that the Library shall make it available to borrowers under rules of the Library.

If I have indicated my intention to copyright this thesis by including a copyright notice page, copying is allowable only for scholarly purposes, consistent with "fair use" as prescribed in the U.S. Copyright Law. Requests for permission for extended quotation from or reproduction of this thesis in whole or in parts may be granted only by the copyright holder.

Natalie Monique Campos

May 2008

ACKNOWLEDGEMENTS

I would like to extend my deepest gratitude to my major advisor, Rick Lawrence, for his constant support and unlimited patience. I would also like to thank Brian McGlynn and Kathy Hansen for the guidance and input. I am especially thankful to Brian McGlynn and Kirstin Gardner for providing the funding for this project and for allowing me to contribute to their research program. I would also like to thank EPA STAR Understanding Ecological Thresholds in Aquatic Systems through Retrospective Analysis – Grant #R832449, Seed funding NSF - Geography and Hydrology Programs (joint funding) - ALSM high resolution topography data acquisition - BCS [0518429](#), Montana Department of Environmental Quality - Science to inform the TMDL process, and USGS 104b Montana seed grant program for their funding. I also want to extend my gratitude to Anne Loi for saving my data from numerous system failures. Most of all, I want to thank my three little munchkin angels for being the driving force behind my ambition.

TABLE OF CONTENTS

1. INTRODUCTION	1
2. LITERATURE REVIEW	3
Mountain Resort Development	3
High-Resolution Imagery Classification.....	5
Object-Oriented Classification	6
Image Fusion	11
Moderate Resolution Change Detection Methods.....	13
Summary	16
3. OBJECT-ORIENTED LAND COVER/LAND USE MAPPING OF MOUNTAIN RESORT DEVELOPMENT	18
Introduction	18
Methods.....	20
Results.....	26
Discussion	32
Object Segmentation.....	32
The Quickbird Classification.....	36
The Fused Classification	38
Conclusion.....	40
4. LAND USE /LAND COVER CHANGE IN BIG SKY, MT: 1990-2005.....	42
Introduction	42
Methods.....	45
Summary of Methods.....	46
Results.....	52
Classification	52
Change Detection.....	54
Spatial Pattern Analysis	55
Discussion	61
Multi-resolution Image Classification	61
Analysis of Temporal Change	63
Conclusion.....	65
5. CONCLUSION	67
LITERATURE CITED.....	71

LIST OF TABLES

Table	Page
3.1 Classification Hierarchy	24
3.2: Error Matrix for Quickbird Classification Level One.....	27
3.3: User's and Producer's Accuracies for Quickbird Classification Level One	27
3.4: Error Matrix for Quickbird Classification Level Two	28
3.5: User's and Producer's Accuracies for Quickbird Classification Level Two	29
3.6: Error Matrix for Fused Classification Level One	29
3.7: User's and Producer's Accuracies for Fused Classification Level One	30
3.8: Error Matrix for Fused Classification Level Two	31
3.9: User's and Producer's Accuracies for Fused Classification Level Two.....	31
4.1: Table of classification scheme for years 1990, 2005, and change image	51
4.2: Error matrix for 1990 Landsat TM classification.....	53
4.3: User's and producer's accuracy for 1990 Landsat TM classification.....	54
4.4: Percentage of each change class to the total amount of change between 1990- 2005.....	56
4.5: Land cover percentages in 1990 Landsat classification.....	56
4.6: Mean value for indicator variables for from-to change change classes	56
4.7: Table of mean and standard deviation values for the indicator variable slope, for forest and grasslands.	57
4.8: Table of mean and standard deviation values for the indicator variable distance-to-roads for forest and grasslands	57
4.9: Table of mean and standard deviation values for the indicator variable distance-to-stream for forest and grasslands.....	58

LIST OF TABLES – CONTINUED

Table	Page
4.10: Proportion of forest and grassland for nine different aspects to the overall amount of forest and grassland in their classification	58

LIST OF FIGURES

Figure	Page
3.1: Study area	21
3.2: Difference between fused and Quickbird classifications	33
3.3: Comparison of Quickbird false color composite and fused classifications showing mixed land cover objects.....	35
3.4: Fused classification showing effects of subsetting images due to memory limitations	36
3.5: Quickbird false color composite and Quickbird classification level Two showing same area	37
3.6: Comparison of false color composite and fused classification.....	38
4.1: Study area	46
4.2: Classified 1990 Landsat TM image based on 2005 Quickbird classification	53
4.3: Classified NDVI difference image showing temporal from-to change classes.....	55
4.4: Classification tree results	60
4.5: Classification tree based classified map of from-to changes	61

ABSTRACT

The goal of this study was to map current and historical development patterns in Big Sky, Montana. Object-oriented classifications of a high-resolution Quickbird image and a fused Quickbird and LiDAR image were compared. Results demonstrated that object-oriented classification can be used to overcome the difficulty associated with pixel-based classification of high-resolution images through the addition of contextual metrics to the classification process. The fused classification resulted in decreased errors of commission and omission for each class, but the differences between the classifications were not statistically significant. The fused classification represented the shapes of land cover objects more precisely based on visual assessment.

Temporal analysis of land cover patterns was accomplished successfully by using a generalized version of the fused classification to map historical development. Previous research on multitemporal mapping of multiresolution images has been lacking. Our research showed that the generalization of a high-resolution classification can be used as training data for a historical image. Normalized Difference Vegetation Index (NDVI) image differencing and boosted classification trees were used to identify and classify areas of change. This resulted in the successful identification of temporal changes in land cover due to Mountain Resort Development (MRD).

Statistical pattern analysis revealed correlations between MRD and the variables distance-to-streams, distance-to-roads, slope, and aspect. Forest changes were found to be disproportionately located farther away from streams and on lower slopes. Grassland changes disproportionately occurred closer to streams, but overall grassland change was proportional to grassland land cover in 1990. Classification tree analysis indicated the variables distance-to-streams, distance-to-roads, slope, and aspect explained 87% of the variance for the change classes and might be related to amenity development. There was an increase in impervious surfaces and a decrease in both forests and grassland areas between the years 1990-2005. Loss of forest and grassland area can result in increased habitat fragmentation and can have negative consequences for ecosystems within the areas. Overall, this project successfully mapped both current and historical development patterns in Big Sky, Montana. This allowed for statistical pattern analysis of variables that have been shown to be correlated with MRD.

CHAPTER 1

INTRODUCTION

Mountain resort development (MRD) is rapidly increasing throughout the Intermountain West. Population growth in the Greater Yellowstone Ecosystem (GYE), for example, has increased 55% between 1970 and 1997 (Hansen et al., 2002). Studies have shown that the main attraction to the intermountain west is the quality of life associated with living near areas rich with natural amenities (Williams and McMillan, 1983; Williams and Jobes, 1990).

The emerging pattern of development is a shift from a primary extractive economy to a tertiary economy. Rural land in the intermountain west is now being converted to residential land for bedroom communities for large mountain resorts and for “ranchette” type development with mountain scrubland and forested areas being most often affected by residential development (Riebsame et al., 1996; Odell et al., 2003). The result of MRD is changes in land use and land cover (LULC), which can affect ecosystems within the developed area, adjoining undeveloped areas, and downstream and riparian systems

The location of MRD relative to wild and semi-wild areas can have important effects on ecological processes and wildlife diversity by causing increased development of the surrounding region as the population grows and demands for services increase (Baron et al., 2000). Rapid development often results in environmental degradation specifically related to waste water disposal (Brown et al., 1997). Despite the possible

implications of MRD on water resources, there has been a lack of research in this area (Shanley and Wemple, 2002).

Remote sensing has the potential to be a valuable tool for analyzing MRD and changes in LULC over time. The synoptic nature of remote sensing might enable efficient mapping of overall MRD patterns. Historical archives of remotely sensed data, in some cases extending over more than three decades, might enable temporal analysis of LULC change patterns.

Big Sky, Montana, provides a valuable opportunity to assess LULC associated with MRD. The first ski resort in the area was established in 1973 with the expansion of the tourism industry taking place entirely within the history of the United States Land Remote Sensing Program. This coincidence in time of development and imagery archives allows for a full examination of development from inception to the current state of extensive development and rapid growth.

CHAPTER 2

LITERATURE REVIEW

Mountain Resort Development

The possible ecological effects of MRD are numerous and wide ranging. Wilderness trails and human development have been found to negatively affect bird communities by changing species composition, resulting in a loss of native species and an increase in generalized species (Miller et al., 1998; Odell et al., 2003). Native birds have also been found to nest less often near trails and have a greater predation rate (Miller et al., 1998).

Tourism pressure increases as mountain resorts become popular destinations, resulting in greater impacts to the environment. It has been found that recreational use impacts, such as litter, plant damage, and fire rings, have negative effects on visitor experiences (Lynn and Brown, 2003). Human activities also change vegetation structure and distribution which in turn affect animal species richness and abundance (Sauvajot et al., 1998). The addition of ski runs, for example, results in destroyed vegetation and increased soil erosion due to vegetation loss (Ries, 1996).

Accessibility has been touted as a primary growth factor for tourism in mountain areas (Price, 2002). The creation of infrastructure creates accessibility pathways that free tourism from ecological constraints and allow access into more remote areas furthering MRD (Price, 2002). The addition of roads and other accessibility pathways increase

habitat fragmentation by splitting larger parcels of land into smaller ones, thereby increasing the overall amount of edge habitats (Reed et al., 1996).

Habitat fragmentation and isolation has been found to be an important predictor of mammalian predator distribution and abundance (Crooks, 2002). Habitat fragmentation affects wildlife by decreasing the area needed for home ranges, foraging, and dispersal patterns (Weaver et al., 1996). Fragmented habitats result in carnivorous mammals having a higher rate of contact with human settlements than less fragmented areas (Crooks, 2002).

The development of tourism in mountain areas is not steady overtime. It has been found that there are varying periods of slow growth often followed by rapid growth (Price, 2002). On a yearly time scale there is also seasonal variation in tourism that affects the economy through increased or decreased revenue and employment (Price, 2002). Mountain resorts facilities often need to be maintained year-round, creating jobs in rural or remote locations and increasing the demand for infrastructure and services.

Development near water has great implications for hydrologic systems. It has been found that the addition of roads affects watersheds by increasing drainage density (Wemple et al., 1996). The temporal development of transportation networks has also been shown to correspond to temporal changes in watershed peak flow patterns (Wemple et al., 1996). Increases in sediment production due to erosion and deposition processes have also been attributed to transportation networks (Wemple et al., 2001). Anthropogenic changes in land cover affect water qualities both in the immediate area and downstream. Harmful ground water nitrate concentrations have been statistically

related to the number of septic tanks found in an area, for example (Gardener and Vogel, 2005).

High-Resolution Imagery Classification

High-resolution imagery provides a detailed look at the land's surface. The Quickbird high-resolution satellite has 2.4-m multispectral resolution at nadir with four bands located in the visible and near-infrared portion of the electromagnetic spectrum. This high spatial resolution allows individual objects to be visually recognized, such as a house or a stand of trees, and is ideal for mapping local areas (Sawaya et al., 2003).

The classification of MRD using high-resolution imagery is difficult due to the complexity found within the scene. LULC associated with MRD is often characterized by high density residential and commercial development, fringe suburban development, outdoor recreation areas such as ski slopes and hiking trails, and natural landscapes such as alpine forests and rock outcrops.

Urban development is the most complex environment to classify due to its composition of houses, roads, vegetation, and commercial development, including structures and parking lots. It has been found that high-resolution sensors lack the spectral capability to capture within class spectral variance of the urban land cover due to their large band width and position within the electromagnetic spectrum (Herold et al., 2003). Investigations on the spectral properties of urban areas found that there were large amounts of spectral variation between features such as roads and rooftops that can only

be distinguished with narrow band intervals (Herold et al., 2004). The spectral variability between features makes per-pixel classifications based on spectral response difficult.

The high-resolution sensors' inability to capture the subtle characteristics of the urban environment results in confusion among classes with similar spectral characteristics in the visible and near-infrared portions of the spectrum such as water and asphalt (Sawaya et al., 2003). The spatial detail of high-resolution sensors also adds shadows from tall objects such as trees and large buildings, which further complicates classification by obscuring the information within the shadow. Object-oriented classification, as opposed to a traditional per-pixel based classification, has been recommended to overcome classification obstacles (Sawaya et al., 2003, Herold et al., 2003)

Object-Oriented Classification

Object-oriented classification differs from pixel based classification methods in that it classifies based on homogenous, spatially contiguous groups of pixels or objects rather than individual pixels. The process begins by segmenting an image into homogenous regions or objects based on user defined parameters such as scale of heterogeneity, shape, compactness, and smoothness. The key to the segmentation process is the creation of semantically meaningful objects, meaning objects resemble their real world counterparts. Objects need to “as large as possible and as fine as necessary” (Definiens Professional 5: LDH, 2007). Once appropriate objects are created contextual metrics such as shape, texture, and location can be calculated and used in their

classification; thus increasing the information extracted from the image (Benz et al., 2003).

The benefits of using an object-oriented classification are numerous. The “simultaneous vector and raster representation” of objects allows for compatibility with GIS systems (Benz et al., 2003). This allows for the integration of GIS information into the classification scheme in the form of ancillary data or the exportation of the classification into GIS systems for further spatial analysis and mapping purposes. Object-oriented classification has also been found to visually improve classification by reducing the pixilation effect found with other classification methods (Carleer and Wolff, 2006).

Object-oriented classification was used to successfully map urban land cover using high-resolution IKONOS imagery of Santa Barbara, California (Herold et al., 2002). Land cover classes included: green vegetation, red tile roofs, light tile roofs, dark roofs, streets/parking lots, swimming pools, natural water bodies, and bare soil/non-photosynthetic vegetation. Overall accuracy was 79%, with individual class accuracies of 95%, 96%, and 92% for green vegetation, swimming pools, and water bodies, respectively (Herold et al., 2002). Low class accuracies for dark roofs and streets/parking lots, 69% and 68%, were direct results of spectral similarity due to similar composition (Herold et al., 2002). The ability to obtain any separation between these two spectrally similar classes was due to the object-oriented classification’s inclusion.

Object-oriented analysis was also used to overcome the spectral similarity of burned and shadowed areas (Mitri and Gitas, 2004). The object-oriented classification in

conjunction with fuzzy logic resulted in overall classification accuracies of 99% for a topographically-corrected image (Mitri and Gitas, 2004). The high overall accuracy highlighted the effectiveness of using an object-oriented classification to overcome spectral similarity.

Object-oriented analysis was used to assess forest conditions of a managed forest in central Japan (Shiba and Itaya, 1996). This study focused on using high-resolution multispectral IKONOS data (Bands 2, 3, and 4), a derived NDVI image, and slope and aspect data derived from a 50-m digital terrain model in the segmentation process (Shiba and Itaya, 1996). The result of analysis was a segmentation based on forest conditions for which management practices could be based upon (Shiba and Itaya, 1996).

Forest inventory parameters were extracted using object-oriented image analysis using IKONOS 2 data in conjunction with Alberta's Vegetation Inventory data and a 10-m x 10-m DEM as ancillary data for a mature forested ecosystem (Chubey et al., 2006). A decision tree classification algorithm was used to create a land cover classification with eight classes: pine-dominant, spruce-dominant aspen-dominant shrub land, grassland, rock, sand, and water (Chubey et al., 2006). The overall accuracy was 93% (Chubey et al., 2006). Individual class accuracy's varied from 81% to 100% with spruce dominant having the lowest accuracy and sand the highest (Chubey et al., 2006).

Object-oriented analysis was used to identify woody vegetation in an urban area of Phoenix, Nevada using high resolution color photography (Walker and Briggs, 2007). The object-oriented classification was used to create a binary classification of woody vegetation (shrubs and trees) and non-woody vegetation (Walker and Briggs, 2007). This

study found that in a fine segmentation objects tended to have similar shape prosperities. This prevented the use of shape characteristics in classification and identification of woody vegetation (Walker and Briggs, 2007). The texture measures were also similar across objects and resulted in a classification based solely on the spectral metrics. The use of object-oriented analysis and classification resulted in an overall accuracy of 81% (Walker and Briggs, 2007).

Object-oriented and pixel-based classifications were compared in a study which attempted to map impervious surface areas (Yuan and Bauer, 2006). A Quickbird image was used to classify five classes: impervious surface, forest, water, non-forested rural, and shadow, in both the object-oriented and the per-pixel classifications (Yuan and Bauer, 2006). These classes were then recoded so as to result in a binary classification of impervious and non-impervious surfaces (Yuan and Bauer, 2006). Results of this study indicate the object-oriented classification had a 1% increase in accuracy over the pixel based classification with accuracy of 94% for the binary classification (Yuan and Bauer, 2006). Although the difference between the classification's accuracy was not substantial, the five class classification's overall accuracy was markedly higher with a 93 % over the pixel-based accuracy of 87% (Yuan and Bauer, 2006).

Object-oriented analysis was also used in a study which attempted to classify mangrove species composition (Wang et al., 2004). Three different classification algorithms were used in the study: a pixel based Maximum Likelihood (ML), a Nearest Neighbor (NN) found within the Definiens Professional software, and a combined ML and NN (MLNN) (Wang et al., 2004). The MLNN was performed by merging the

spectrally similar classes into one class and performing a ML classification. The spectrally similar classes were masked and then imported to the object-oriented software where it was segmented and classified using the NN algorithm (Wang et al., 2004). The results of the study indicated that the combined MLNN classification had the highest accuracy with 91% and a Kappa statistic of 0.81 (Wang et al., 2004). The pixel based ML had an overall accuracy of 89% with a Kappa of 0.73 (Wang et al., 2004). The NN had an overall accuracy of 80%, with a Kappa of 0.94 (Wang et al., 2004). The decrease in accuracy for the NN classification was attributed to the misclassification of one particular mangrove species, which had a decrease in accuracy of 76% (Wang et al., 2004). The increase in Kappa is a result in an increase in individual class accuracies for three mangrove species which had low class accuracies with the ML classification (Wang et al., 2004).

Classification methods are becoming more complex as the use of object-oriented analysis becomes more prevalent. Object-oriented analysis and pixel based classifications were also compared in a deforestation study of Rondonia, Brazil (Budreski et al., 2007). The Cart[®] 5.0 and a *k*-Nearest Neighbor (*k*-NN) algorithm were used on a temporal series of Landsat images in order to map three different land uses: primary forests, cleared, and regrowth (Budreski et al., 2007). Results from this study indicated that there was no statistically significant difference between the accuracies of the pixel or segmentation based classifications (Budreski et al., 2007).

Object-oriented analysis has also been used to map benthic habitats using aerial photography for a portion of Texas's gulf coast region (Green and Lopez, 2007). The

study area was first subset into 6 geographic regions prior to analysis and segmented to create objects related to different benthic habitats (Green and Lopez, 2007). Classification of the objects was achieved through the use of classification and regression tree analysis in the See5 software package (Green and Lopez, 2007). The overall accuracy for this project was 74% (Green and Lopez, 2007). Individual classes with low accuracies were used to identify between class confusion and used to gather more field reference data to be used in the manual editing of the classification (Green and Lopez, 2007). This resulted in an overall accuracy of 90% (Green and Lopez, 2007).

Image Fusion

The purpose of image fusion is to combine information from different sensors in order to increase the information extracted (Pohl and Van Genderen, 1998). There are many examples of image fusion. Panchromatic images have been fused with multi-spectral images to create images with increased spatial resolution. Different multi-spectral sensors, such as Landsat and SPOT, have been fused in order to increase radiometric resolution. Active and passive sensors, such as LiDAR and multi-spectral sensors, have been fused to create images with both spectral and elevation information.

The utility of data fusion was examined in a study that compared the accuracy of fused images to single sensor images (Hyde et al., 2006). That study found fused images had the highest accuracy when estimating maximum and mean canopy heights (Hyde et al., 2006). The higher R^2 for fused data set is related to the increase in information provided by the combination of spectral and height information. Fused ETM+ data

achieved a higher R^2 than fused Quickbird data due to ETM+'s additional bands and a wider range within the electromagnetic spectrum. This allows ETM+ to contribute more information to the classification.

LiDAR and multi-spectral data fusion was also used to investigate accuracy differences between fused and individual sensor data sets for estimating canopy height and stem density (McCombs et al., 2003). Results showed that live individual tree identification for low-density plots had a higher accuracy for the fused image than LiDAR alone (McCombs et al., 2003). High-density live individual tree identification plots also had a higher accuracy for the fused data set than LiDAR alone, but were substantially less accurate than the low-density plots (McCombs et al., 2003). Tree height was best represented by LiDAR, which underestimated tree height by 0.15-m on average for high-density and 0.38-m for low-density, while the fused data underestimated tree height by 0.42-m for high and 0.5-m for low-density plots (McCombs et al., 2003).

The combination of LiDAR and hyper-spectral data also has been used to create a thematic map related to the National Vegetation Classification for Woodlands and Scrubs in the United Kingdom (Hill and Thomson, 2005). The map was created by combining the first two principal components of 12 selected bands from the HyMap sensor and a digital canopy height model derived from LiDAR first returns (Hill and Thomson, 2005). The resulting image was then segmented into parcels and used to create a thematic map with 10 distinct classes relating to species composition and canopy height that could not have been produced using any one sensor (Hill and Thomson, 2005). The combination of

the LiDAR canopy height model and the two principal components allowed the subtle differences between vegetation types to be captured and accurately classed.

The utility of data fusion has not been limited to vegetation studies. It has been used in conjunction with color infrared aerial images to extract buildings and trees from urban environments (Haala and Brenner, 1999). Data was fused by using a normalized digital surface model from the laser altimeter data as an additional band in classification resulting in each pixel having height information. This allowed height attributes to be used in classification, increasing the accuracy of extracted buildings and trees (Haala and Brenner, 1999).

Fused data sets have also been used with object-oriented classifications. One study used a pan-sharpened Quickbird image and object-oriented classification in order to map fractional vegetation cover of urban environments (Moeller, and Blaschke, 2006). The original 2.4 multispectral pixels were merged with the 0.6 panchromatic band via the IHS (Intensity – Hue – Saturation) algorithm (Moeller and Blaschke, 2006). This resulted in an image with 0.61 spatial resolutions and the spectral information of the 4 original bands (Moeller and Blaschke, 2006). The resulting object-oriented classification resulted in an overall accuracy of 83% (Moeller and Blaschke, 2006).

Moderate Resolution Change Detection Methods

Change detection is the processes of identifying temporal changes in a pixel's digital brightness value and associating the change with corresponding biophysical

changes in land cover. Change detection algorithms are as numerous as possible change detection applications and vary in complexity.

Image differencing is a relatively simple change detection algorithm. It is performed by subtracting an image of one date from an image of another date, resulting in an image with no change centered on the mean and change identified in the tails of the distribution. Image differencing is one of the most commonly used change detection techniques and has been recommended for binary change/non change purposes (Lu et al., 2003). The simplicity of image differencing is its main advantage, and when used with vegetation indices the spectral response of features is emphasized (Lu et al., 2003). The disadvantage of image differencing is that it does not provide from-to information and like CVA requires the selection of a threshold in order to capture change (Lu et al., 2003). Image differencing was used successfully to identify areas of degradation and regeneration in the tropical forests of Venezuela using the Modified Soil Adjusted Vegetation Index (MSAVI) (Guerra et al., 1998). It was found that MSAVI differences between the two dates were a result of vegetation changes due to swidden agricultural practices (Guerra et al., 1998).

Principal Component Analysis (PCA) has also been recommended for binary change/non-change purposes (Lu et al., 2003). A significant advantage of PCA is its ability to reduce band redundancy (Lu et al., 2003). A significant disadvantage of PCA is that it is data dependent and can be difficult to interpret and classify (Lu et al., 2003). Principal Component Analysis (PCA) has been used to monitor land use change due to rapid urban expansion in China's Pearl River Delta (Li and Yeh, 1998). Change was

identified by performing PCA on a radiometric and geometrically corrected multi-date stacked image (Li and Yeh, 1998). Final analysis was performed by using a maximum likelihood classification on the first four principal components, which contained 97% of the variance (Li and Yeh, 1998).

Change Vector Analysis (CVA) identifies and quantifies change through the magnitude and movement of a pixel in spectral space (Johnson and Kasischke, 1998). This results in the creation of unique and discrete change vectors that can then be categorized as change from-to. CVA requires preprocessing, such as radiometric normalization and accurate image-to-image registration in order to avoid spurious change identification (Johnson and Kasischke, 1998). A significant advantage of CVA is its ability to process any number of bands. CVA has been successfully used to monitor forest disturbance and re-growth in the Great Smoky Mountain by monitoring pixel movement and magnitude of change in tasseled cap feature space (Allen and Kupfer, 2000). CVA has also been used to monitor LULC changes related to vegetation dynamic in the GYE) over a period of 20 years (Paramenter et al., 2003).

Many studies have compared the accuracy and effectiveness of different change detection methods. One study compared the ability of four different change detection methods, image differencing, image regression, tasseled cap differencing and a chi square transformation, for identifying change from no change (Ridd and Liu, 1998). The different methods were applied band by band resulting in 15 change images (Ridd and Liu, 1998). The chi square transformation uses information from the six Landsat reflective bands and resulted in a single change image (Ridd and Liu, 1998). The 16 total

change images were compared and results indicated differencing Landsat's red band had the highest accuracy (Ridd and Liu, 1998). Results also indicated image differencing and image regression were both effective and performed similarly when using the visible bands to identify change (Ridd and Liu, 1998).

The use of Artificial Neural Networks (ANN) for change detection has also been investigated (Liu and Lathrop, 2002). ANNs are machine learning algorithms which like other classifiers, require the use of training and test data in order to extract accurate information from the input data. This study focused on the comparison of ANNs and post-classification comparison as well as an investigation on the optimal input for the classification of from-to urban change (Liu and Lathrop, 2002). Six bands (excluding thermal) from each of two anniversary date Landsat images were used as inputs for one classification while the first three principal components from each date were used in a separate classification (Liu and Lathrop, 2002). Results indicate that classification based on the principal component input had the highest accuracy (Liu and Lathrop, 2002). When comparing the use of ANNs and post-classification comparison ANN had a higher accuracy than post-classification comparison, mainly due to compound error associated with post classification comparison (Liu and Lathrop, 2002).

Summary

MRD in Big Sky, Montana can be attributed to the creation of mountain resorts and the attraction of living in an area rich with natural amenities. LULC changes associated with MRD affect the native flora and fauna of the area and can affect water

quality and other physical processes. The use of object-oriented classification in conjunction with high-resolution satellite imagery and LiDAR might be used to create detailed LULC maps to inventory the current distribution of LULC in Big Sky, Montana. Change detection methods might then be used to assess change in the historical distribution of LULC over time.

CHAPTER 3

OBJECT-ORIENTED LAND USE/LAND COVER MAPPING OF MOUNTAIN
RESORT DEVELOPMENTIntroduction

Mountain resort development (MRD) is rapidly increasing throughout the intermountain West (Hansen et al., 2002). MRD generally results in land use and land cover (LULC) change, which can affect ecosystems within the developed area, adjoining undeveloped areas, and downstream and riparian systems. The location of MRD relative to wild and semi-wild areas can have important effects on ecological processes and wildlife diversity (Baron et al., 2000).

MRD has been found to be spurred by the creation of transportation networks (Price, 2002). Transportation networks can negatively affect watershed processes (Wemple et al., 1996; Wemple et al., 2001). Roads and wilderness trails have been found to affect species composition and increase habitat fragmentation (Miller et al., 1998; Reed et al., 1996). Habitat fragmentation is an important predictor of species distribution and abundance (Crooks, 2002).

MRD needs to be accurately mapped in order to assess and monitor the quantity and extent of MRD. The use of object-oriented classification and analysis of high-resolution imagery is advantageous for mapping land use/land cover (LULC) associated with MRD. High-resolution imagery provides a detailed view of the land's surface and is important for mapping local areas (Sawaya et al., 2003). Traditional pixel-based

classification of high-resolution imagery has been difficult due the lack of spectral depth of most high-resolution sensors (Herold et al., 2003; Herold et al., 2004). Object-oriented classification and analysis can overcome pixel-based classification problems by allowing users to classify based on contextual information extracted from an image in addition to spectral characteristics (Benz et al., 2003).

Many recent studies have investigated the use of object-oriented analysis for LULC classification. The spectral similarity of burned and shadowed areas was successfully distinguished through the use of object-oriented classification with an accuracy of 99% (Mitri and Gitas, 2004). The high overall accuracy highlighted the effectiveness of object-oriented classification in overcoming spectral similarity. Object-oriented classification has also been used to temporally monitor vegetation changes in the southwestern United States (Laliberte et al., 2004). Results indicate that the addition of spatial information derived from object-based analysis approximates human logic but benefits through the addition of automation (Laliberte et al., 2004). Object-oriented analysis has also been used to identify woody vegetation in urban areas based solely on mean spectral values (Walker and Briggs, 2007). The spatial or contextual information was not used in the classification process due to objects having no distinct shape pattern or texture. The segmentation process in that study, however, did create homogenous objects and resulted in an overall accuracy of 81%.

Image fusion might also increase the accuracy of object-oriented classification and analysis. The purpose of image fusion is to combine information from different sensors in order to increase the information extracted (Pohl and Van Genderen, 1998).

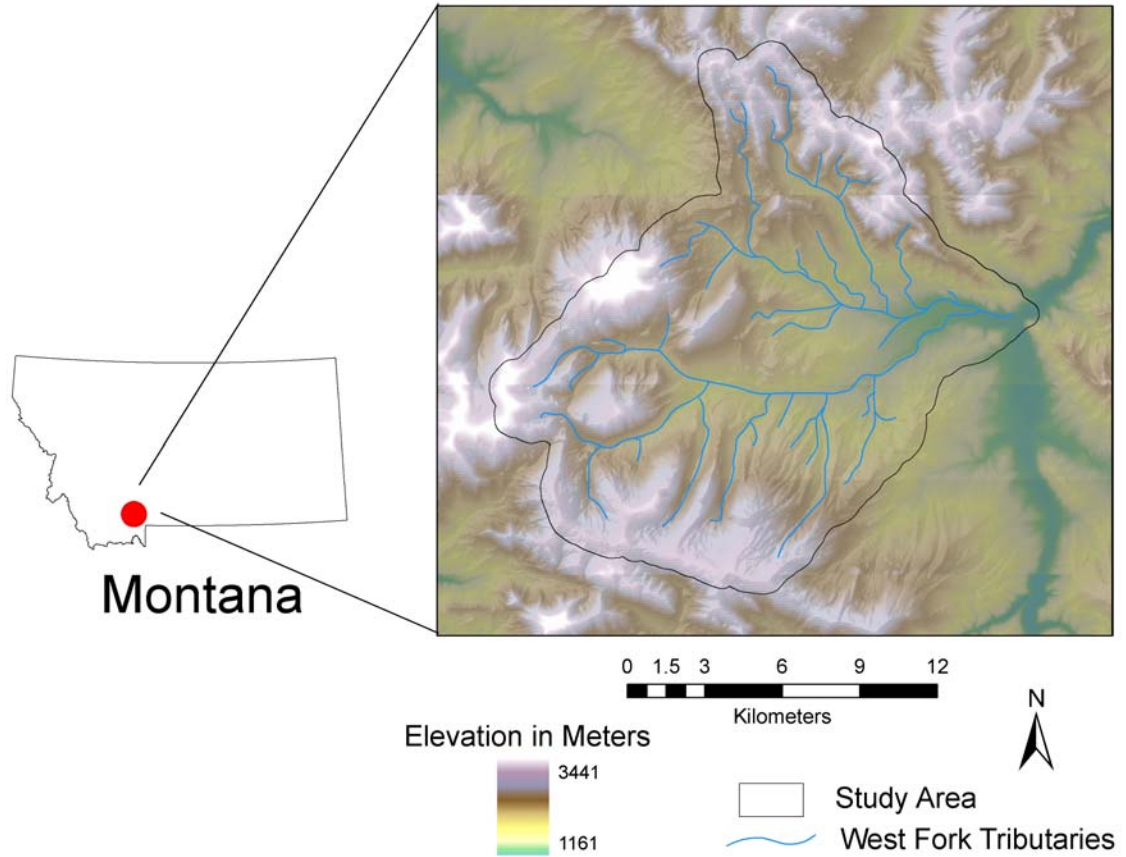
The fusion of LiDAR and multispectral images has been shown to increase the accuracy of forest parameter estimations as compared to single sensors (Hyde et al., 2006; McCombs et al., 2003). Fused LiDAR and hyper-spectral data have also been used to map vegetation species composition and distribution (Hill and Thomson, 2005). The utility of data fusion has not been limited to vegetation studies. The extraction of buildings and trees from urban environments has been accomplished through the use of fused aerial photographs and laser altimeter data, which allowed height to be used in classification and increase the accuracy (Haala and Brenner, 1999).

The purpose of this study was to evaluate the utility of high-spatial-resolution imagery fused with airborne laser swath mapping, herein referred to as LiDAR, to map LULC associated with MRD using object-oriented analysis. Results were compared with object-oriented analysis in the absence of LiDAR data.

Methods

The study area for this project was the West Fork of the Gallatin River watershed near Big Sky, Montana (Figure 3.1). The study area comprised 24091.3 ha. Big Sky is surrounded by the Gallatin National Forest in southwestern Montana and is located within the Greater Yellowstone Ecosystem (Marston and Anderson, 1991). Elevation ranges more than 2000-m and is an important predictor of climate and vegetation species distribution (Marston and Anderson, 1991). Vegetation is composed of coniferous forests, shrublands, and grasslands. Frost free days range from 60-90 and decrease with increased altitude (Parmenter et al., 2003; Marston and Anderson, 1991).

Figure 3.1: Location of West Fork of Gallatin River watershed study area to the state of Montana. The study area boundary is shown in black and the West Fork tributaries are shown in blue.



Imagery used for the study included an 11-tile Quickbird image with 2.4-m spatial resolution. A tile represents the 16.5 km x 16.5 km footprint of the sensor containing only the portion of the scene related to the study area with all outlying areas containing no data. The Quickbird image contained 4 bands in the visible and near infrared (NIR) portion of the electromagnetic spectrum including blue (450-520 nm), green (520-600 nm), red (630-690 nm), and NIR (760-900 nm). The 11 tiles were mosaicked to create one master image.

1-m LiDAR bare earth and surface models created from point clouds were also used. The bare earth model was created through triangulation of the last returns in a 55-m window (NCLAM processing report, 2005). The surface model was created using a linear Kriging algorithm to interpolate first returns in a 5-m window. Both models were exported to ESRI Arcinfo GRID format. The surface model represented surface land cover, such as the top of tree canopies and the roofs of buildings. The bare earth model estimated elevation with all land cover (e.g., vegetation and buildings) removed. The Lidar images were resampled to 2 m using nearest neighbor resampling. All images, Quickbird and LiDAR, were acquired in the summer of 2005 and registered to a UTM NAD 83 Zone 12 projection with an RMSE of 0.06.

The original 11 tiles of Quickbird imagery were used to create six image subsets. Subsetting was necessary due to data processing limitations within the object-oriented software. The six subsets were then used to create matching subsets of the resampled LiDAR bare earth and surface models. The subsets were then imported into the Definiens Professional 5: Large Data Handling (LDH) software (Definiens Professional 5: LDH, 2007). The Quickbird and LiDAR fused data created data sets with multispectral, bare-earth elevation, and surface information for each pixel.

The subsets were initially segmented using a Multi-Resolution Segmentation (MRS) algorithm (Definiens Professional 5: LDH, 2007). Separate segmentations were created for each subset with and without LiDAR data. The MRS algorithm is a heuristically applied algorithm that creates objects by minimizing internal object heterogeneity. Object heterogeneity is calculated as a weighted average across all input

bands with the total weight summing to one. Object heterogeneity is controlled by selecting an arbitrary scale factor, which determines the amount of heterogeneity acceptable and is resolution dependant. The scale factor required to create objects for individual houses will be different than the scale factor required to create objects representing a neighborhood or subdivision, for example. The appropriate object is one that is “as large as possible and as fine as necessary” and thus will vary depending on the desired output (Definiens Professional 5: LDH, 2007). The segmentation process resulted in vector based “objects” with attributes corresponding to the mean and standard deviation values of the pixels within the object for each input layer. Additional contextual metrics can then be calculated and used in the classification process. The appropriate MRS was determined if object borders did not overlap different LULC classes by visual inspection.

The creation of objects is also influenced by weighting layer pixel values and spatial homogeneity. The default was a pixel value weight of 0.9 and a spatial weight of 0.1 (Definiens Professional 5: LDH, 2007). A decrease in pixel input value weight and a corresponding increase in spatial weight results in objects with less similarity in their pixel values. The default spectral and spatial weights were chosen because they provided objects that followed spectral contrast lines for different land cover by visual inspection.

A Spectral Difference Segmentation (SDS) was performed after the appropriate MRS was identified (Definiens Professional 5: LDH, 2007). SDS is a merging algorithm designed to merge spectrally similar objects produced in previous segmentations. Objects were merged if their standard deviation was below a user defined threshold. The

threshold is used to determine the amount of object aggregation. The appropriate SDS was identified if most or all adjacent objects were merged without creating mixed land cover objects. This resulted in larger objects, which were more semantically meaningful.

A hierarchical classification scheme was used in this study (Table 3.1). This study was part of a larger study examining the effect of MRD on stream nitrogen levels, and the primary interest was to distinguish impervious surfaces from other specified land cover types. We sought to determine in addition, however, whether our approach could also distinguish various impervious surface types. Waste water holding ponds and golf courses represent thematic areas that were manually digitized at the end of the classification process.

Table 3.1: Classification hierarchy for fused and non-fused images level one and level two.

Level One	Level Two
Impervious Surfaces	Roads
	Building
	Rock
Bare Soil	Bare Soil
Golf Course	Golf Course
Vegetation Not Tree	Vegetation Not Tree
Lake/Pond	Lake/Pond
Waste Water Holding Pond	Waste Water Holding Pond
Shadow	Shadow
Snow	Snow
Tree	Tree
River/Stream	River/Stream

Classification of objects was conducted using the nearest neighbor (NN) algorithm in Definiens Professional. The NN algorithm classifies objects based on user

identified sample objects utilizing user selected metrics. Metric selection was determined using Definiens' Feature Space Optimization tool (FSO). FSO works by examining any number of input variables and identifying the variables that contain the greatest distance between samples to be applied to the NN classifier.

The following pixel derived metrics were selected by FSO: object mean and standard deviation of all input bands excluding blue (green, red, NIR, NDVI, surface, and bare earth). NDVI is a commonly used vegetation index that is calculated as $(\text{NIR} - \text{red}) / (\text{NIR} + \text{red})$ (Rouse et al., 1973). NDVI is a unitless measure with a positive correlation to vegetation amount or health. The following contextual metrics were used: length/width, asymmetry, density, compactness, and rectangular fit.

Training samples were chosen by selecting objects in each image that represented their class. Additional training objects were added to improve misclassified classes and new classifications were conducted until improvements in classification rates were minimal. Definiens Professional allowed the sample metrics collected in one image to be applied to subsequent images. This allowed the sample metrics collected in the first subset to be applied in the classification of subsequent subsets. Once all 12 subsets were classified, they were mosaicked to create two final classifications, a Quickbird classification and a fused LiDAR and Quickbird classification.

The fused classification required additional post processing due to missing data values within the LiDAR image. This was overcome by applying the Quickbird classified values to the missing data.

The vector based classification was converted to a raster image with 2.4-m pixel resolution to retain the spatial properties of the original Quickbird data. A total of 1126 accuracy assessment points were generated using a stratified random sample from the Quickbird classification. An additional 609 stratified random sample points were obtained from the fused classification. The two sets of points were merged and used to assess the accuracy of both classifications. Producer's and user's accuracies for each class and the Kappa statistics were calculated for each classification (Congalton and Green, 1999). Overall accuracy was calculated using the methods outlined in Carrao et al., 2007. This method differs from the traditional overall accuracy, in that it is calculated based on the relative proportion of each class to the total number of classified pixels.

Results

The overall accuracy for the Quickbird classification level one was 90% with a Kappa statistic of 0.78 (Table 3.2). The bare soil class had the lowest user's and producer's accuracy and was often confused with impervious surfaces (Table 3.3). The error of omission for bare soil was 72%, meaning that 72% of the bare soil pixels were not classified as such. The error of commission relates to what percentage of the classified pixels was actually the class they were classified. Grass had a high error of commission rate with 35%, meaning 35% of the pixels were classified as grass but were not. Grass was confused with impervious surfaces and trees. The river, shadow, and snow classes each performed similarly with a low producer's accuracy and high user's

accuracy. Impervious surface, lakes/ponds, and trees all achieved user's and producer's accuracies over 85%.

Table 3.2: Error Matrix for Quickbird Classification Level One.

	Bare Soil	Impervious	Grass	Lake	River	Shadow	Snow	Tree	Row Total
Bare Soil	35	12	2	0	0	0	0	4	53
Impervious	39	589	8	0	0	12	30	8	686
Grass	45	31	168	1	1	0	0	12	258
Lake	0	2	0	46	1	0	0	0	49
River	0	0	0	0	17	0	0	0	17
Shadow	0	0	0	0	0	52	0	0	52
Snow	2	3	0	1	0	0	73	2	81
Tree	6	31	11	4	6	5	2	474	539
Column Total	127	668	189	52	25	69	105	500	1735

Overall Classification Accuracy = 90%

Overall Kappa Statistic = 0.78

Table 3.3: User's and Producer's Accuracies for Quickbird Classification Level One.

Class Name	Reference Pixel Totals	Classified Pixel Totals	Number Correct	Producer's Accuracy	User's Accuracy
Bare Soil	127	53	35	28%	66%
Impervious	668	685	588	88%	86%
Grass	0	1	0	89%	65%
Lake	189	258	168	88%	94%
River	52	49	46	68%	100%
Shadow	69	52	52	75%	100%
Snow	105	81	73	70%	90%
Tree	500	539	474	95%	88%

The Quickbird classification level two achieved an overall accuracy of 90% with a Kappa statistic of 0.76 (Table 3.4). All individual class user's and producer's accuracies remain the same except for the expansion of the impervious class into buildings, rocks, and roads (Table 3.4). The building class had a low error of commission as seen in the high user's accuracy but also had a higher error of omission as seen in the low producer's accuracy. The road class had a higher error of commission than omission. The rock class had a high error of commission with 35% and a moderate error of omission with 11%.

Table 3.4: Error Matrix for Quickbird Classification Level Two.

	Bare Soil	Building	Grass	Lake	River	Road	Rock	Shadow	Snow	Tree	Row Total
Bare Soil	35	1	2	0	0	10	1	0	0	4	53
Buildings	0	131	0	0	0	4	1	0	0	0	136
Grass	45	11	168	1	1	12	9	0	0	12	259
Lake	0	0	0	47	1	0	1	0	0	0	49
River	0	0	0	0	17	0	0	0	0	0	17
Road	20	48	0	0	0	202	3	0	0	1	274
Rock	19	5	8	0	0	13	181	12	30	7	275
Shadow	0	0	0	0	0	0	0	52	0	0	52
Snow	2	1	0	1	0	0	2	0	73	2	81
Tree	6	19	11	4	6	7	5	5	2	474	539
Column Total	127	216	189	53	25	248	203	69	105	500	1735

Overall Classification Accuracy = 90%

Overall Kappa Statistic = 0.76

Table 3.5: User's and Producer's Accuracies for Quickbird Classification Level Two.

Class Name	Reference Total	Classified Total	Number Correct	Producer's Accuracy	User's Accuracy
Building	216	136	131	61%	96%
Road	248	274	202	81%	74%
Rock	203	275	181	89%	66%

The fused classification level one had an overall accuracy of 91% and a Kappa statistic of 0.8 (Table 3.6). Bare soil had similar error rates to the Quickbird classification (Table 3.7). The error of omission for bare soil, however, increased over the Quickbird classification level one. All other individual user's and producer's accuracy were generally higher than the Quickbird classification resulting in reduced errors of omission and commission.

Table 3.6: Error Matrix for Fused Classification Level One.

	Bare Soil	Impervious	Grass	Lake	River	Shadow	Snow	Tree	Row Total
Bare Soil	19	2	0	0	0	0	0	0	21
Impervious	57	608	5	0	0	2	14	10	696
Grass	45	37	172	2	0	0	4	19	279
Lake	0	2	0	47	1	0	0	0	50
River	0	0	0	0	21	0	0	0	21
Shadow	0	0	0	2	0	62	0	0	64
Snow	2	6	1	0	0	0	86	2	97
Tree	4	13	11	1	3	5	1	469	507
Column Total	127	668	189	52	25	69	105	500	1735

Overall Classification Accuracy = 91%

Overall Kappa Statistic = 0.8

Table 3.7: User's and Producer's Accuracies for Fused Classification Level One.

Class Name	Reference Totals	Classified Totals	Number Correct	Producer's Accuracy	User's Accuracy
Bare Soil	127	21	19	15%	90%
Impervious	668	696	608	91%	87%
Grass	189	279	172	91%	62%
Lake	52	50	47	90%	94%
River	25	21	21	84%	100%
Shadow	69	64	62	90%	97%
Snow	105	97	86	82%	89%
Tree	500	507	469	94%	93%

Overall accuracy for the fused classification level two was 91% with a kappa statistic of 0.78 (Table 3.8). The expansion of the impervious class resulted in buildings having a 16% decrease in error of omission than the Quickbird classification and a slight 1% decrease in error of commission (Table 3.9). The road class had a 5% decrease in error of commission with the fused classification and no increase in the error of omission. The rock class had slight decreases in both errors of omission and commission than in the Quickbird classification.

Table 3.8: Error Matrix for Fused Classification Level Two.

	Bare Soil	Building	Grass	Lake	River	Road	Rock	Shadow	Snow	Tree	Row Total
Bare Soil	19	1	0	0	0	1	0	0	0	0	21
Building	1	166	0	2	0	4	0	0	0	0	173
Grass	45	12	172	10	0	18	7	0	4	19	287
Lake	0	0	0	37	1	0	1	0	0	0	39
River	0	0	0	0	19	0	0	0	0	0	19
Road	24	27	0	1	0	202	1	0	1	0	256
Rock	32	4	5	0	0	20	184	2	13	10	270
Shadow	0	0	0	2	1	0	0	62	0	0	65
Snow	2	1	1	0	0	0	5	0	86	2	97
Tree	4	5	11	1	4	3	5	5	1	469	508
Column Total	127	216	189	53	25	248	203	69	105	500	1735

Overall Classification Accuracy = 91%

Overall Kappa Statistic = 0.78

Table 3.9: User's and Producer's Accuracies for Fused Classification Level Two.

Class Name	Reference Totals	Classified Totals	Number Correct	Producer's Accuracy	User's Accuracy
Building	216	173	166	77%	96%
Road	248	256	202	81%	79%
Rock	203	270	184	91%	68%

Each classification was compared to its counterpart, the fused classification versus the Quickbird classification, in order to determine if any statistical difference between the two existed. It was found that neither the level one nor the level two classifications had any statistical differences in Kappa statistics (Congalton and Green, 1999). The z statistic for the level one classification was 1.13 and 1.06 for level two (p-values = 0.02), both are below the critical value of 1.96 at an alpha of 0.05 (Congalton and Green, 1999).

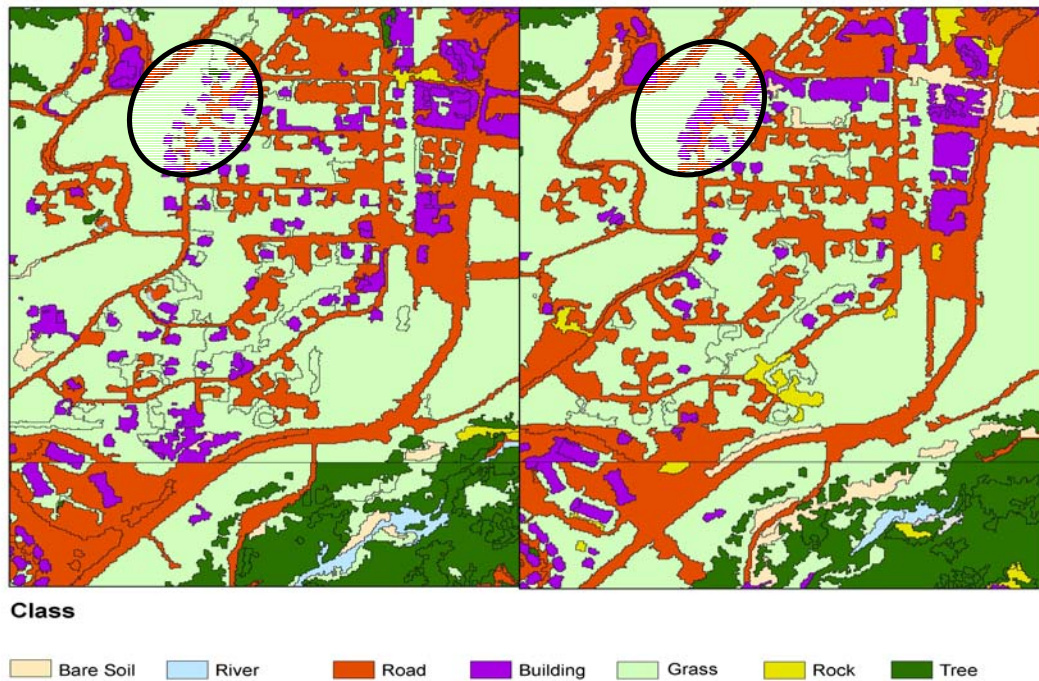
Discussion

Object Segmentation

The segmentation process was successful in the creation of semantically meaningful objects. Houses were easily identified in both segmentations and generally resulted in independent objects. This allowed contextual information in addition to spectral and elevation information to be used in the classification. The key for the segmentation process was the creation of homogeneous objects. This was achieved through the heuristic nature and application of the MRS and SDS segmentation algorithms. The results were objects that represented their land cover class spectrally and contextually.

The use of the surface and elevation models resulted in objects that appeared to better reflect surface features compared to using Quickbird imagery alone (Figure 3.2). The addition of elevation information in the fused classification resulted in many more objects than the Quickbird classification. This allowed smaller patches of land cover to be identified and objects to have a much more distinguishable shape. Dense housing, for example, in the Quickbird classification was block shaped, while the same area in the fused classification had individual houses that were shaped similar to their physical structure (Figure 3.2).

Figure 3.2: Difference between fused (left) and Quickbird (right) classifications.



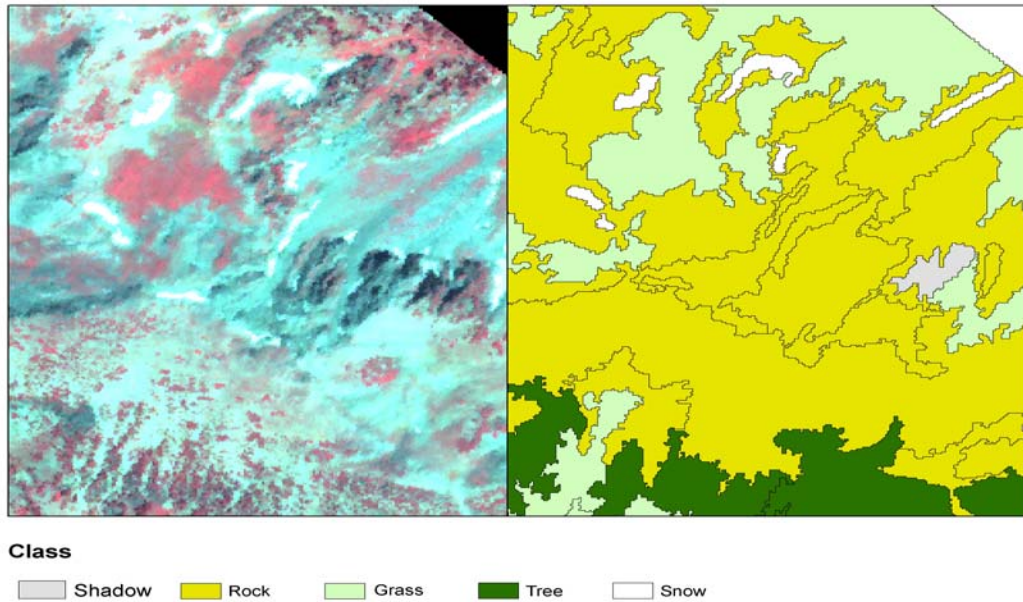
The issue of scale presented a problem for the segmentation process. Previous studies have focused on the use of homogenous landscape regions such as primarily urban or natural areas (Chubey et al., 2006; Laliberte et. al., 2004; Walker and Briggs, 2007; Budreski et al., 2007). These studies have shown the successful use of object-oriented classification and analysis, but have not explored the use for heterogeneous landscapes. There were two major land cover types within our study area, developed and undeveloped. Developed land cover consisted of road networks and buildings. Undeveloped land cover consisted of grassland, river/stream, lake/pond, and forested areas. These types have different levels of appropriate segmentation. The appropriate level of segmentation to create an object representing a house will be smaller than the level needed for forests or grasslands. An intermediate segmentation scale was used as a

compromise in order to create objects “as large as possible and as fine as necessary” (Definiens Reference Book, 2005, p. 11).

Mixed land cover objects caused difficulty in the selection of class samples. Samples that represented their class while still capturing the variability of their class were selected. This required the selection of some mixed land cover objects as samples of the dominant land cover they contained. The spectral attributes of an object were the means of all pixels it was composed of for each input. Mixed land cover objects, therefore, skew the distribution of the response for the dominate land cover they represent. This is a likely explanation of misclassification rates (Figure 3.3). Objects that were predominately impervious also tended to have small patches of vegetation, for example.

Point-based accuracy assessment does not account for mixed land cover objects. Thus, true accuracy is unknown. Point-based accuracy only accounts for what is on the ground at one particular point. Points located on the edges of objects or part of a mixed land cover objects could inflate error rates and lead lower accuracies. New methods of calculating overall accuracy are needed for full evaluation of object-oriented analysis.

Figure 3.3: Comparison of Quickbird false color composite and fused classifications showing mixed land cover objects.

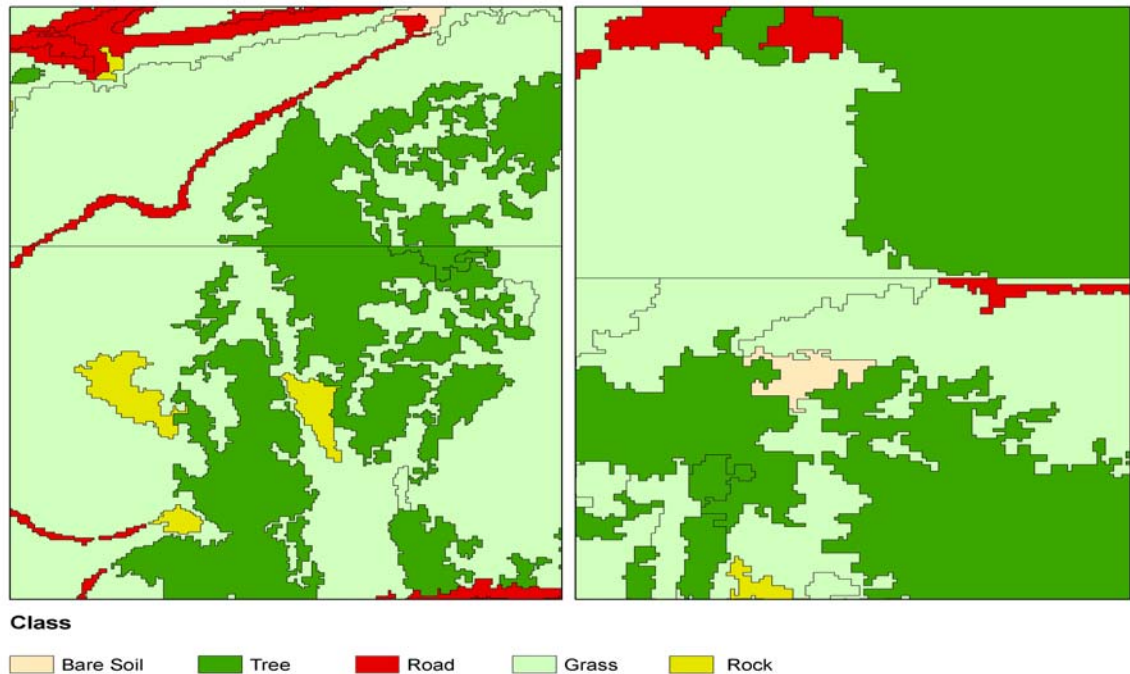


Transition zones created difficulties in both classifications. Bare earth and grass are not discrete land cover types, for example. They often flow between each other with varying intensity. This caused difficulty with the creation of distinct boundaries and resulted in the low accuracy for the bare soil class.

The object-oriented software was memory intensive and had data processing limitations. High-spatial-resolution images contain large numbers of pixels for spatially small areas. The Quickbird full image was 64 MB and the LiDAR image was 1.7 GB. The software used could not handle the file sizes and therefore required subsetting the data and resampling the LiDAR data. This created objects that did not always flow between subsets (Figure 3.4). A study that mapped benthic habitat on the Gulf Coast of Texas also needed to resample their 1-m aerial photographs and subset their study into several smaller portions (Green and Lopez, 2007). Other studies have focused on the use

of small, less computationally demanding areas (Chubey et al., 2006; Laliberte et al., 2004; Walker and Briggs, 2007; Budreski et al., 2007; Benz et al., 2003).

Figure 3.4: Fused classification showing effects of subsetting the images due to memory limitations.

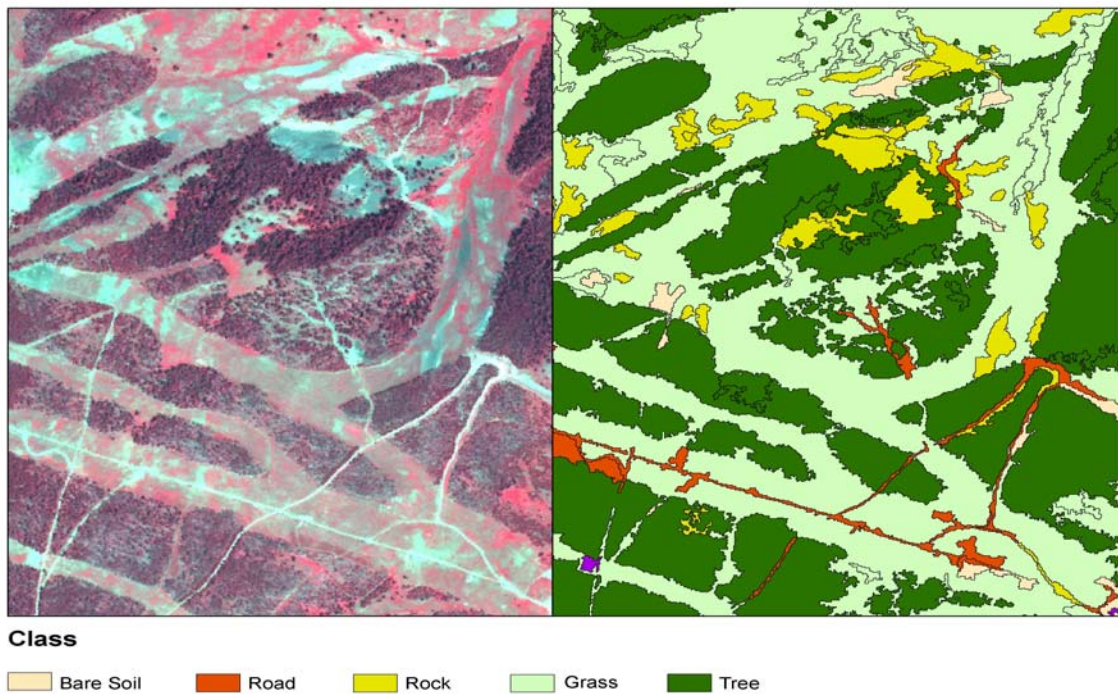


The Quickbird Classification

Overall accuracy for the Quickbird classification was high at 90% for both level one and level two. Previous studies have found the lack of spectral depth of high-resolution sensor makes pixel-based classification difficult (Sawaya et al., 2003). Classes such as roads, shadows, and water bodies have had high misclassification rates with traditional pixel-based classification (Sawaya et al., 2003; Herold et al., 2003). Object-oriented classification in our study was able to overcome this through the addition of the contextual metrics to the classification process.

The Quickbird classification had difficulties with several classes. The bare ground class, for example, was often misclassified as impervious surface or grass. This was a result of the continuous nature of bare soil and the creation of discrete boundaries. Small patches of bare soil were often contained in larger objects of impervious surface or grass (Figure 3.5). The impervious surface classes were also confused with forest and grass. Similar to the bare ground class, misclassification can be attributed to small patches not being identified.

Figure 3.5: Quickbird false color composite and Quickbird classification level two showing same area.



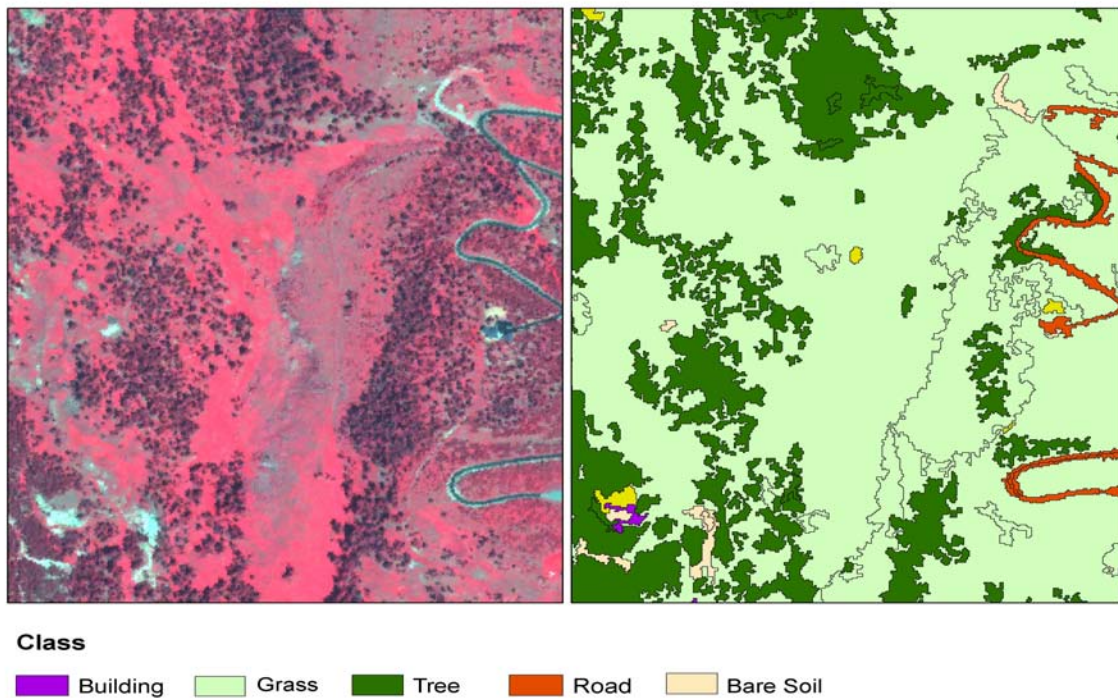
Previous studies on the use of object-oriented classification have found similar results. One study mapped densely populated areas of Santa Barbara, California with an overall accuracy of 79% (Herold et al., 2002). Another study mapped an area of mixed residential and agriculture land cover with an overall accuracy of 74% (van der Sande et

al., 2003). Both studies found that roads or building classes had confusion (Herold et al., 2002; van der Sande et al., 2003). This was mostly a result of the two classes not being separated in the segmentation process, as seen in our classification. Our classification had confusion with bare soil and grass. This was overcome in one study by the use of broad classes such as non-photosynthetic vegetation/bare soil and general photosynthetic vegetation (Herold et al., 2002).

The Fused Classification

The accuracy of the fused classification was slightly higher than the Quickbird classification, but no significant differences were found. The additional information of the elevation and surface models resulted in the segmentation creating objects that better reflected surface objects by adding contrast in areas of spectrally low contrast (Figure 3.6). This can be seen in the creation of objects representing small groups of trees and small patches of bare soil. The Kappa statistic did not have a statistically significant increase, but the estimated overall accuracy and Kappa statistic were higher. This is consistent with our observations that the differences were represented by more accurate delineation of objects, although the total area affected by these differences was small. Individual class user's and producer's accuracy also improved for many of the classes, thus reducing the error of commission and omission.

Figure 3.6: Comparison of false color composite and fused classification.



The fused classification had similar accuracy difficulties as the Quickbird. Bare soil had a high rate of misclassification with impervious surfaces and grass. Impervious surfaces had a high confusion with grass. Snow also had a high misclassification rate with impervious surfaces. These errors can be attributed to the creation of discrete boundaries for continuous land cover types. Overall, the fused classification had higher consistency, as there were less dramatic differences between the user's and producer's accuracies than seen in the Quickbird classification.

Previous studies have used image fusion with topographic data with great success. Studies have compared image fusion to single sensors and found that image fusion results in increased accuracy for pixel based classifications due to the inclusion of elevation information to the classification process (Hyde et al., 2006; McCombs et al., 2003; Hill and Thomson, 2005). Our results show little improvement in overall accuracy when

compared with the Quickbird classification. This is a result of the success and power of the segmentation processing in creating objects, which can be accurately classified through the addition of contextual metrics. The addition of the LiDAR resulted in finer objects, which reduced error rates but did not improve overall accuracy.

Conclusion

Object-oriented analysis and classification works well with high-resolution imagery. Object-oriented classification can overcome the traditional spectral limitations of high-resolution sensors. The appropriate segmentation level coupled with the addition of contextual metrics can accurately create detailed maps. Object-oriented classification can be used to map accurately heterogeneous land cover areas such as dense urban areas, rural or suburban areas, and natural land cover.

Image fusion and object-oriented classification creates realistic objects. This results in a classification that is more visually appealing. This is advantageous if spatial precision required, but might not be necessary if only point-based accuracy is needed.

There are a plethora of future research opportunities for object-oriented classification and analysis. One significant research area includes identification of an appropriate spatial resolution for use with object-oriented classification and analysis. Quickbird imagery has high spatial resolution but is still pixilated, which blurs the boundaries of different land cover. Increased class accuracy and homogenous objects might be achieved in future research if the optimum spatial resolution was identified.

Another research area would be the full utilization of contextual metrics. The Definiens Professional software allows for an extreme number of metrics to be calculated, including standard deviations and ratios of both spectral and contextual metrics. This is a new frontier in image classification, as most of these have not been tested for relevance or relation to different LULC classes. These new metrics need to be researched and identified, as has been done for NDVI, for use in the classification of objects.

Object-oriented software also needs to be programmed so as to make full use of today's high resolution data. Today's technology is resulting in an increased number of sensors with increasing spatial resolution. This software's inability to work with large data sets relegates it to a novelty procedure not currently useful for landscape-scale classification.

CHAPTER 4

LAND USE /LAND COVER CHANGE IN BIG SKY, MT: 1990-2005

Introduction

Mountain Resort Development (MRD) is rapidly increasing throughout the intermountain west. The result is changes in land use and land cover (LULC), which can affect ecosystems within the developed area, adjoining undeveloped areas, and downstream and associated riparian systems.

The conversion of naturally vegetated land to impervious surfaces, such as roads, can have dramatic effects. Roads have been found to increase habitat fragmentation (Reed et al., 1996). Habitat fragmentation in turn has been found to decrease species composition distribution and abundance (Odell et al., 2003; Crooks, 2002; Miller et al., 1998). Roads also affect physical processes. Roads have been shown to increase drainage density and sediment production due to erosion and deposition (Wemple et al., 2001; Wemple et al., 1996).

Understanding the variables associated with potential causes of LULC change due to MRD is important in order to mitigate its effects. Accessibility has been named as a primary growth factor for tourism in mountain areas (Price, 2002). We would expect, therefore, that MRD would be correlated to roads within a watershed.

Other studies have shown that the quality of life associated with living near areas rich with natural amenities is a significant attraction for development in rural areas (Williams and McMillan, 1983; Williams and Jobes, 1990). Amenity development often

results in the conversion of rural land to residential land for “ranchette” type development (Riebsame et al., 1996; Odell et al., 2003). Topography and water area are important variables and have been considered the basis of a “natural amenity index” (Cromartie and Wardell, 1999). Evaluation of MRD with respect to topographic variables is also important because of its effects on watershed processes. Increased development on steeper slopes, for example, might increase rates of erosion and related impacts of aquatic ecosystems (Wemple et al., 2001; Groffman et al., 2003).

Remote sensing has the potential to be a valuable tool for analyzing MRD and changes in LULC over time. The use of remote sensing for identification of LULC change has been well documented (Coppin et al., 2004; Mas, 1999). Change detection algorithms are as numerous as possible applications and vary in complexity.

Many studies have compared the accuracy and effectiveness of various change detection methods. Univariate image differencing has been recommended for binary change/non-change identification (Coppin et al., 2004; Lu et al., 2003). The use of vegetation indexes for change detection also has been shown to be advantageous over single band analysis, because it reduces data volume and captures information not available in any single band (Coppin et al., 2004). Normalized Difference Vegetation Index (NDVI) image differencing has been shown to be advantageous over the use of other vegetation indexes for identification of deforestation and vegetation loss and has also been shown to be less affected than other indexes by topographic relief (Lyon et al., 1998). This makes NDVI image differencing an ideal candidate for binary change/no-

change identification related to MRD where we are examining the clearing of natural habitats for anthropogenic development in an area of high relief.

Classification of from-to change is imperative, once change has been identified, in order to discern development patterns. Classification tree (CT) methods are becoming increasingly popular for classification of remotely sensed data and might be useful for such from-to change. CTs have been shown to create more accurate classifications than other methods (De'ath and Fabricius, 2000). CTs offer the advantages of being non-parametric, working equally well with continuous and nominal data types, producing interpretable rule sets, and handling noisy data sets (Friedl and Brodley, 1997). CT, therefore, offers significant advantages over other classification methods; however, they can be negatively affected by the presence of outliers in training data and by unbalanced data sets (Lawrence et al., 2004). Statistical boosting has been shown to significantly increase the accuracy of CTs (Bricklemeyer et al., 2007; Baker 2007; Baker et al., 2006; Lawrence et al., 2004).

Multi-resolution image classification has been shown to increase single image classification accuracy (Moeller and Blaschke, 2006; Hyde et al., 2006; McCombs et al., 2003). Multi-resolution image classification is generally considered a form of image fusion whose purpose is to combine information from different sensors in order to increase the information extracted (Pohl and Van Genderen, 1998). The use of multi-resolution images for change detection purposes, however, does not seem to be as well developed as use for single classifications. This raises a significant issue with modern high-resolution satellite imagery. High-resolution imagery is increasingly being used for

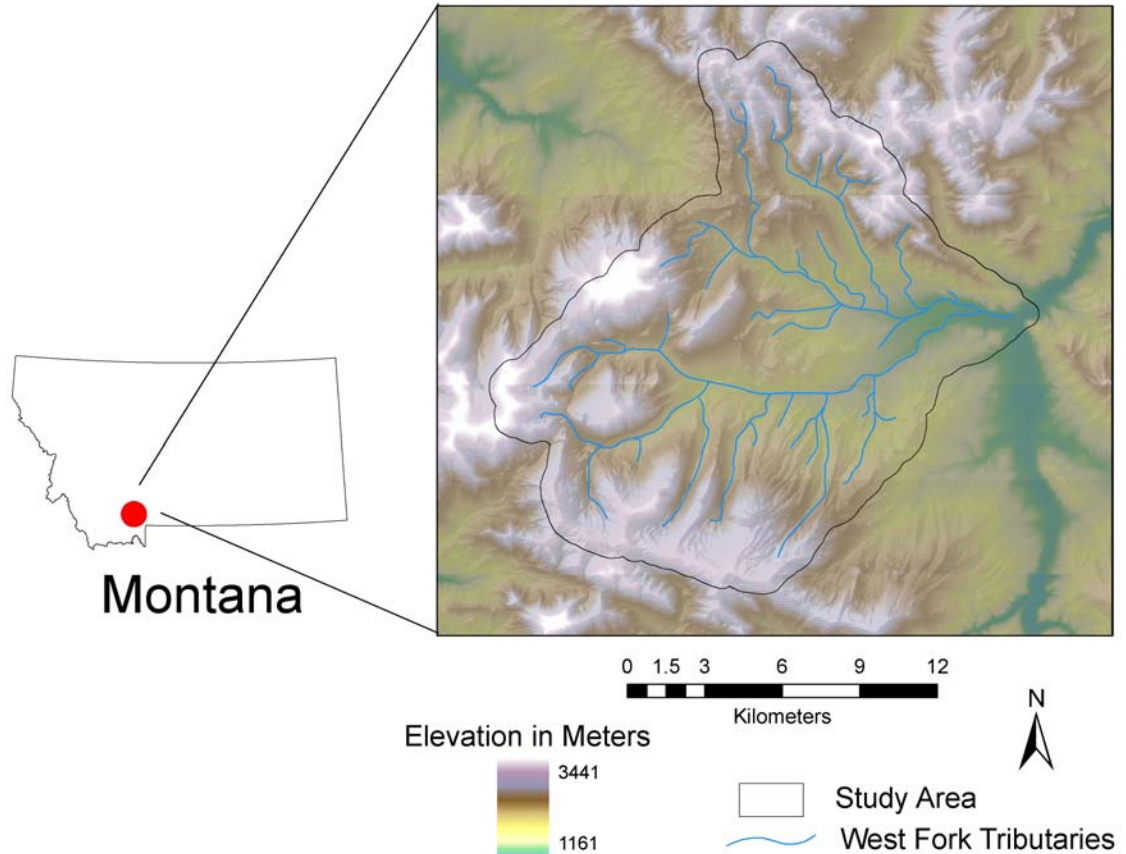
LULC classifications, but the absence of a long-term archive of high-resolution imagery, as exits for moderate-resolution imagery, has made it less useful for LULC change analysis. Development of approaches that fuse high-resolution classifications with moderate-resolution imagery for LULC change analysis would greatly increase the usefulness of high-resolution classifications.

The purpose of this study was to (1) identify LULC change related to MRD in Big Sky, Montana, between the dates of July 2005 and July 1990 using high-resolution imagery from 2005 and moderate resolution imagery from 2005 and 1990 and (2) evaluate topographical variables and spatial relationships to roads and streams as possible correlates of MRD in the area.

Methods

The study area for this project was the West Fork of the Gallatin River watershed near Big Sky, Montana (Figure 4.1). The study area comprised 24091.3 ha. Big Sky is surrounded by the Gallatin National Forest in southwestern Montana and is located within the GYE (Marston and Anderson, 1991). Elevation ranges more than 2000 m and is an important predictor of climate and vegetation species distribution (Marston and Anderson, 1991). Vegetation is composed of coniferous forests, shrublands, and grasslands. Frost free days range from 60-90 and decrease with increased altitude (Parmenter et al., 2003; Marston and Anderson, 1991).

Figure 4.1: Location of West Fork of Gallatin River watershed study area to state of Montana. The study area boundary is shown in black and the West Fork tributaries are shown in blue.



Summary of Methods

Identification of change patterns for statistical analysis was a multistep process. Two normalized near anniversary date Landsat 5 images were converted to NDVI and differenced to identify change from no-change. Classification of from-to change was carried out by first resampling a 2005 Quickbird classification with an accuracy of 91% to 30 m. Identified change locations in the 1990 Landsat image were classified, using the unchanged locations as training data. Changed areas were then combined with the unchanged locations in the 2005 classification to create the final 1990 classification. The

spatial distribution of change was analyzed through a combination of descriptive statistics and CT.

Landsat 5 Thematic Mapper (TM) scenes (path 39 and row 28) from July 12, 2005 and July 3, 1990 images were obtained from EROS Data Center with level one terrain correction. The two scenes were geometrically registered to a July 2005 Quickbird image and set to a UTM NAD 83 Zone 12 projection. The Landsat 1990 image had an RMSE of 0.05 and the 2005 image had a RMSE 0.07. The full scenes were then subset to the study area.

Data transformations were performed on both Landsat dates to provide derived indexes for use in the classification and change detection processes. A tasseled cap transformation was performed. The tasseled cap is a linear transformation of the original six Landsat reflective bands resulting in three new bands representing relative soil brightness, relative amount of green vegetation, and relative soil moisture content (Crist and Cicone, 1984). NDVI was also calculated as $(\text{NIR}-\text{red})/(\text{NIR}+\text{red})$ (Rouse et al., 1973). NDVI is a unitless measure with a positive correlation to vegetation amount or health.

A multi-date image normalization using linear regression was used as a radiometric normalization procedure on the 1990 and 2005 NDVI images (Collins and Woodcock, 1996). The 2005 image was selected as the independent variable and the 1995 image was selected as the response variable. Pseudo-invariant features (PIFs) representing features that were presumed to have not changed over time were identified and selected. Stable anthropogenic features included features that were both bright (e.g.,

buildings) and dark (e.g., man-made water features) and were ideal candidates; an attempt was made to select features in relatively flat areas so as not to introduce topographic effects. A total of 224 points were collected. 100 points were randomly selected and set aside to be used as a validation data set. The R^2 for the NDVI regression model was 0.91 and was shown to be statistically significant (p -values of <0.001).

Paired t-testing was performed in order to determine whether the normalization improved the 1990 image. It was determined that the mean difference between the 2005 and the 1990 image was 7.4 with a standard deviation of 17.2. The mean difference between the 2005 and the normalized 1990 image was 6.1 with a standard deviation of 9.3. The paired t-test indicated that there was a difference between both the 1990 image and the 1990 normalized image and the 2005 image. This difference was decreased, however, with the normalization process.

NDVI image differencing was used for binary change/no-change identification. Image differencing was performed by subtracting the pixel values of the 2005 NDVI image from the pixel values of normalized NDVI 1990 image. The resulting values have no-change centered on the mode and areas of change located in the tails of the distribution. Change was then identified by defining a threshold based on knowledge of certain changed locations to separate areas of change from no-change. The appropriate threshold was identified so as to include all areas of change while minimizing false positive change identification. A binary image of change and no-change was created based on this threshold.

A 30-m resolution 2005 classification was created based on a classified fused Quickbird and LiDAR classification with a resolution of 2.4 m. The original classes of grasslands/shrublands, bare soil, and golf courses were generalized to grasslands/shrublands. Houses, roads, and rock were generalized to impervious surfaces. Lakes, rivers, ponds, streams, and waste water holding ponds were generalized to water. The forest class was generalized to forest. Snow and shadows were left to represent themselves.

The generalized 2.4-m classification was then resampled to 30 m to match the 1990 Landsat image. Resampling was accomplished by determining within each 30-m pixel the most common land cover type present.

The use of the resampled generalized classification resulted in 30-m pixels that represented mixed land cover. This resulted in the loss of important information related to MRD, such as roads and other smaller features. A percent impervious model was created in order to overcome this loss of information by determining within each 30-m pixel the percent of 2.4-m pixels that were impervious, based on the 2.4-m classification. Pixels that were 20% or more impervious were reclassified as impervious for the 30-m classification. This resulted in an overestimation of the impervious class but also decreased the loss of information related to MRD due to resampling.

The NDVI-based change/no-change image was used to separate areas of change and no-change from the 1990 Landsat image. Areas of no-change were used as training for classification of the changed locations. Data used for the 1990 classification consisted of normalized data from all six Landsat reflective bands and derived indexes

(NDVI and TC). The See5 data mining program (RuleQuest, 2008) was used for classification. See5 is a statistical data mining software package that performs CT analysis with boosting. A total of 10 boosts were used. The unchanged 2005 classified pixels were merged with the classified changed 1990 pixels to create a final 1990 classified map.

Accuracy for the 1990 classification was assessed using a stratified random sampling design. A total of 302 sampling points were acquired. An additional 14 points were manually identified because the stratified random design was unable to identify an acceptable number of water points. These were then combined with the stratified random points for a total of 316. These points were then visually compared to 1:40,000-scale aerial photographs from the National Aerial Photography Program (NAPP) archives.

Producer's and user's accuracies for each class and the Kappa statistics were calculated for each classification (Congalton and Green, 1999). Overall accuracy was calculated using the methods outlined in Carrao et al., 2007. This method differs from the traditional overall accuracy (Congalton and Green, 1999), in that it is calculated based on the relative proportion of each class to the total number of classified pixels.

Our data set contained the full population of possible land cover change for our study area. This allowed descriptive statistics to be examined in order to evaluate potential indicators of change in the study area. Four potential indicators were identified: slope, aspect, distance-to-roads, and distance-to-streams. There were 16 theoretically possible from-to change classes. Three of the 16 were identified as possibly being related to MRD (Table 4.1). These were individually coded so as to separate the different types

of change for spatial pattern analysis. Two of the classes represent change from natural habitats to human habitats through the conversion of vegetation to impervious surfaces. Change class FI represented change from forests in 1990 to impervious surfaces 2005. Change class GI represented change from grasslands/shrublands in 1990 to impervious surfaces in 2005. Change class FG represented changes in forests in 1990 to grasslands/shrublands in 2005. A national forest boundary map created by the U.S. Forest Service was used to exclude areas on forest service land where MRD was known not to have occurred.

Table 4.1: Table of classification scheme for years 1990, 2005, and change image.

Classified as in 1990	Classified as in 2005	Change Class
Forests	Impervious Surfaces	FI
Grasslands/Shrublands	Impervious Surfaces	GI
Forests	Grasslands/Shrublands	FG

Slope and aspect were calculated from 1-m LiDAR elevation model resampled to 30 m using the nearest neighbor algorithm. Slope was calculated as degrees and aspect was calculated as a categorical variable representing eight different directions (north, northeast, east, southeast, south, southwest, west, and northwest) and flat. A distance-to-roads layer was created by calculating distance from a road vector file of the area onto a 30-m grid. The road layer was created by the GIS Department of Gallatin County, Montana, and contained all the roads in the study area. This layer is updated twice yearly by Gallatin County and was current as of January 2008. Distance-to-streams represented the topographically-driven flow path distance on a 30-m grid from streams identified by using a single flow direction algorithm on a 10-m parsed elevation model created from the

original 1-m LiDAR elevation model. The 10-m parsed elevation model was created by selecting every 10th point on the 1-m LiDAR model and rescaling to 10 m.

Descriptive statistics were computed relating each type of change to each indicator variable being evaluated. The mean and standard deviation of each type of change for each variable was calculated and compared to the mean and standard deviation of land cover types and variables for the 1990 classification.

CT analysis was used to determine the relative relationship of the potential indicators to the three different types of change. The three change classes were used as the response variables. Slope, aspect, distance-to-streams, and distance-to-roads were used as the explanatory variables. Standard cross validation methods were used to avoid over-fitting the model (Venables and Ripley, 1997).

Results

Classification

The use of the generalized 2005 high-resolution Quickbird classification was successful in the mapping of the 1990 Landsat image (Figure 4.2). The 1990 classification had an overall accuracy of 86% with a Kappa statistic of 0.79 (Table 4.2). All four classes had minimal error rates. Grasslands and forests were most often confused (Table 4.3). Water achieved no error of omission or commission. Impervious surfaces had some confusion with grasslands.

Figure 4.2: Classified 1990 Landsat TM image based on 2005 Quickbird classification.

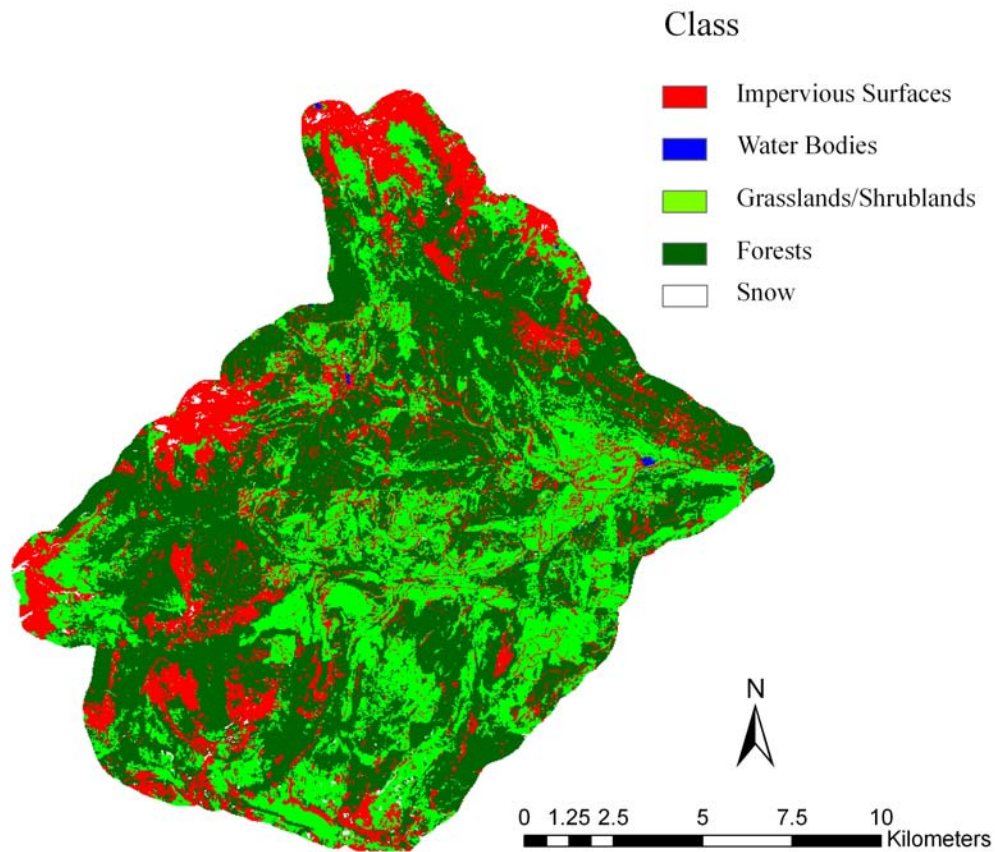


Table 4.2: Error matrix for 1990 Landsat TM classification. Columns represent reference classes, while rows represent how the pixels were classified.

	Grasslands/ Shrublands	Impervious surfaces	Water	Forests
Grasslands/Shrublands	81	5	0	12
Impervious surfaces	0	57	0	0
Water	0	0	14	0
Forests	26	1	0	120

Overall accuracy = 86%

Kappa Statistic = 0.79

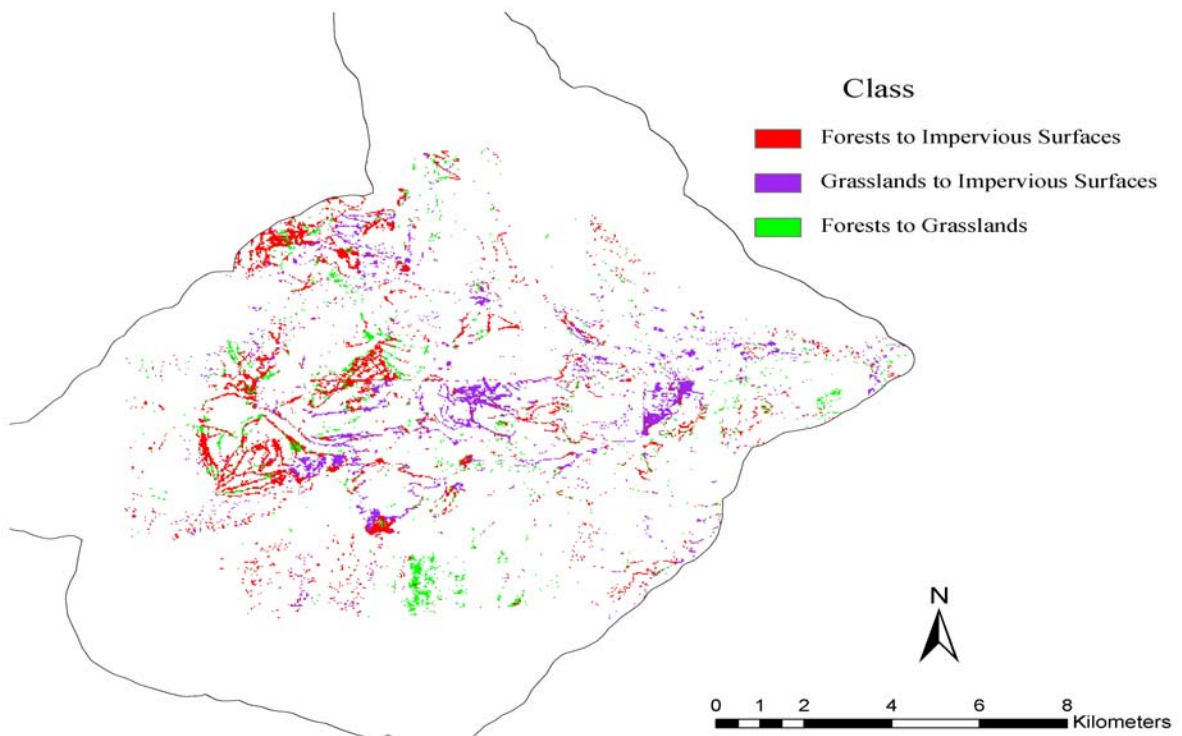
Table 4.3: User's and producer's accuracy for 1990 Landsat TM classification.

Class Name	Producer's Accuracy	User's Accuracy
Grasslands/Shrublands	76%	83%
Impervious surfaces	90%	100%
Water	100%	100%
Forests	91%	82%

Change Detection

NDVI differencing successfully identified change related to MRD in our study area (Figure 4.3). The NDVI differencing method captured patterns of development as seen in the linear patterns and clustering of change pixels around the two major areas of development in Big Sky, the Mountain Village and the Meadow Village. The NDVI differencing method did not result in excessive amounts of false positive change identification. The use of the forest boundary also aided in the minimization of false positive change identification.

Figure 4.3: Classified NDVI difference image showing temporal from-to change classes.



Spatial Pattern Analysis

Analysis of from-to change indicated that the proportion of from-to changes were disproportionate to the original land cover in 1990 (Table 4.4; Table 4.5). Forest change accounted for 67% of the total change between 1990 and 2005. Forest, however, only accounted for 51% of the land cover in 1990. Grassland changes accounted for 33% of the total change and were proportional to its 1990 land cover with 29%.

Table 4.4: Percentage of each change class to the total amount of change between 1990-2005.

Change Class	Percent of Change
FI	48%
FG	19%
GI	33%

Table 4.5: Land cover percentages in 1990 Landsat classification.

Classified as in 1990	Percent of Land Cover in 1990
Grasslands	29%
Impervious Surface	19%
Forest	51%
Water	1%

The three change classes had differences among them for each of the indicator variables. GI had the smallest slope mean followed by FG and FI changes (Table 4.6). The three change classes differed in the mean response for distance-to-roads. GI had the shortest distance followed by FI and FG. FI and FG changes had similar mean values for distance to streams. .

Table 4.6: Mean value for indicator variables for from-to change change classes.

Change Class	Slope	Distance-to-Roads	Distance-to-Streams
FI	14	177.7	646
GI	9.4	90.3	397.3
FG	12.4	337.8	601

The proportion of 1990-2005 land cover changes to the overall proportion of land cover classes in 1990 for each variable was also examined. Mean and standard deviation for slope and grassland change did not differ from the values for grasslands in the 1990 classification (Table 4.7). FI and FG changes were combined in order to investigate overall amount of forest loss. Forest changes occurred on a lower mean slopes than the overall mean forest slopes in the 1990 classification.

Table 4.7: Table of mean and standard deviation values for the indicator variable slope for forest and grasslands. Slope is represented in degrees.

	Mean slope values in 1990 classification	Mean slope value in change classification	Standard deviation of slope in 1990 classification	Standard deviation of slope in change classification
Forests	16.5	13	9.2	8.4
Grasslands	12.5	12.4	8.6	6.8

Mean changes in forests and grasslands were located closer to roads than the mean response of forest and grasslands in the 1990 classification. Both forest and grassland changes averaged 300-m closer to roads than the mean forest and grassland distance in 1990 classification. The standard deviations of forests and grasslands changes were also smaller than the standard deviation of forest and grassland in the 1990 classification (Table 4.8).

Table 4.8: Table of mean and standard deviation values for the indicator variable distance-to-roads for forest and grasslands. Distance-to-roads is represented in meters.

	Mean distance-to-roads values in 1990 classification	Mean distance-to-roads value in change classification	Standard deviation of distance-to-roads in 1990 classification	Standard deviation of distance-to-roads in change classification
Forests	637.7	317	724.7	392.4
Grasslands	397	90.3	624.9	267.8

Changes in forest and grasslands differed in their mean response for distance-to-stream (Table 4.9). Forested change was located farther way from streams than the mean forest distance in the 1990 classification. Grassland change, however, was located closer to streams than the mean grassland distance in the 1990 classification.

Table 4.9: Table of mean and standard deviation values for the indicator variable distance-to-stream for forest and grasslands. Distance-to-stream is represented in meters.

	Mean distance-to-stream values in 1990 classification	Mean distance-to-stream value in change classification	Standard deviation of distance-to-stream in 1990 classification	Standard deviation of distance-to-stream in change classification
Forests	550.7	649.1	400.9	413.9
Grasslands	516.2	397.4	409.3	321.9

The relationship between forest and grassland conversion was also examined with respect to aspect (Table 4.10). The overall proportion of forest change and the proportion of forest in the 1990 classification to aspect were similar. The largest difference between forest change and classified forest in 1990 was in the southeastern direction with 6% less changed than represented in the 1990 classification. Grassland changes in aspect were also similar to the proportion of grassland aspect in the 1990 classification. The largest difference for grasslands was a 5% decrease in grasslands between 1990-2005 in the northwest direction.

Table 4.10: Proportion of forest and grassland for nine different aspects to the overall amount of forest and grassland in their classification.

	Percent of forest change between 1990-2005	Percent of forest class in 1990 classification	Percent of grassland change between 1990-2005	Percent of grassland class in 1990 classification
North	17%	15%	19%	15%
Northeast	20%	17%	19%	17%
East	14%	15%	12%	16%
Southeast	17%	11%	14%	15%
South	10%	10%	12%	13%
Southwest	6%	10%	7%	8%
West	5%	8%	4%	6%
Northwest	11%	14%	13%	8%
Flat	0.001%	0.001%	0.001%	0.001%

The CT based on the cross validation model was able to separate the three types of change (Figure 4.4). The CT model accounted for 87% of the variance within this data set. FI change was separated into four different groups. Three of the groups were located less than 63.5 m from roads while one group was located greater than 63.5 m from roads. GI change was grouped in to three groups, two being closer to roads than the last. All three change classes occurred in areas greater than 63.5 m from roads. FG was captured in a single group of change and was located greater than 63.5 m from roads.

The mapped classification tree displays the spatial patterns of from-to changes (Figure 4.5). Blue shades represent GI changes, red shades represent FI changes, and green represents FG change. Class A represents a dense cluster of GI change. This particular group of change was caused by development of the area known as Meadow Village. FI change due to the creation of ski slope is seen mostly in classes E and H. Class E, however also capture the FI change of Mountain Village. The small amount of FG change can be seen in an area with little development and can be attributed to forest management practices such as logging.

Figure 4.4: Classification tree results. Branch length is proportional to amount of deviance explained. End nodes represent the from-to change class. Nodes were coded alphabetically in order to map their spatial distribution (Figure 4.5).

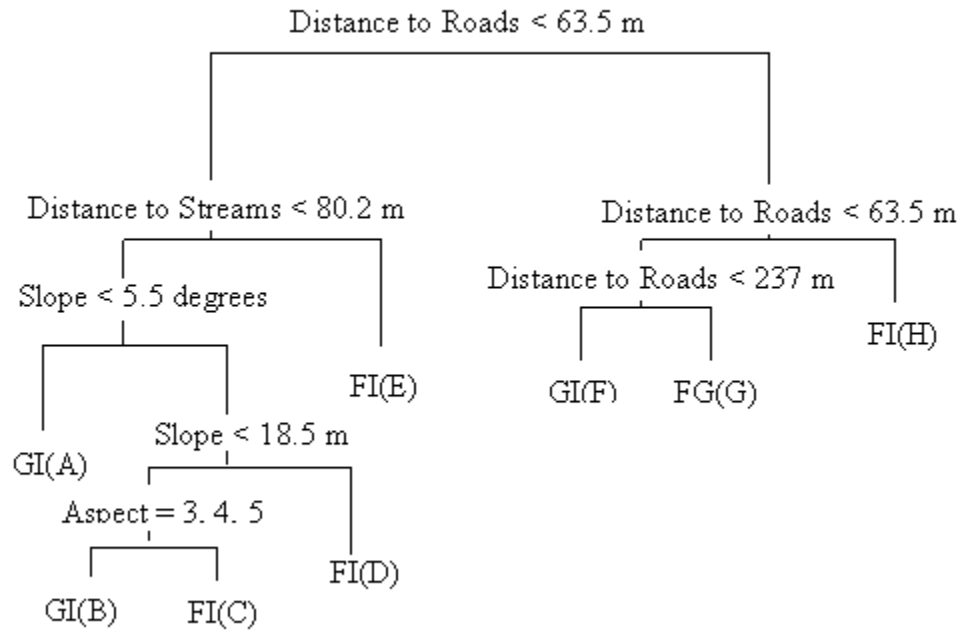
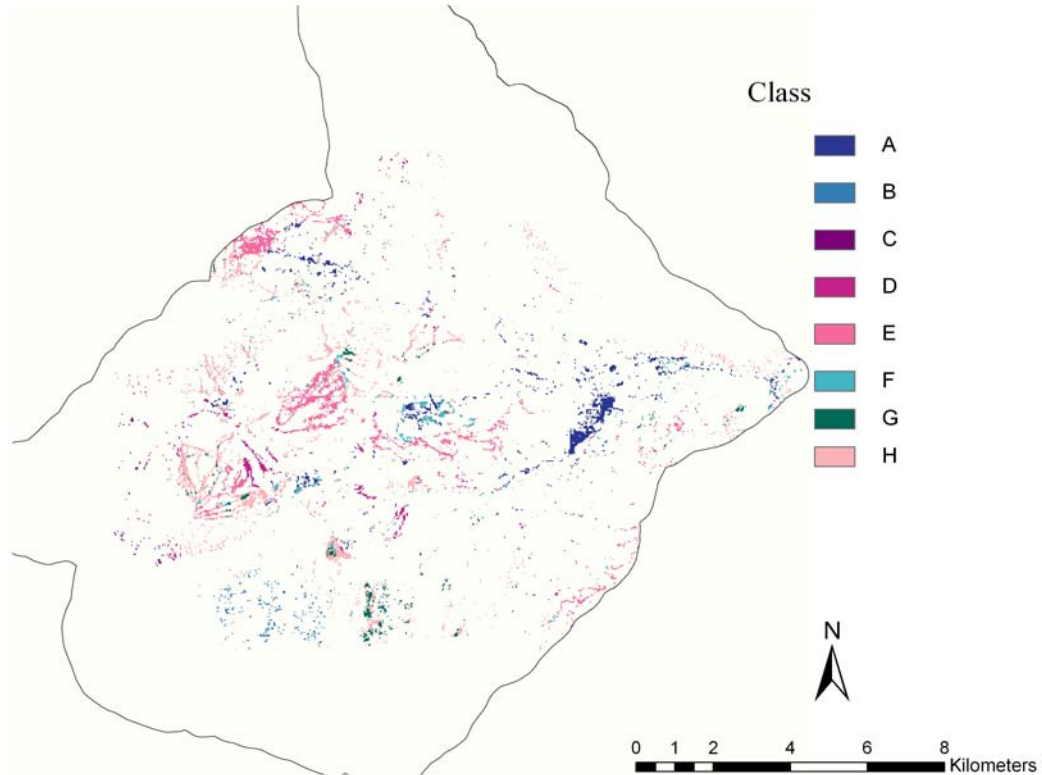


Figure 4.5: Classification tree based classified map of from-to changes. Each class is coded alphabetically to match tree nodes from left to right (Figure 4.4). Blue shades represent GI changes, red shades represent FI changes, and green represents FG change.



Discussion

Multi-resolution Image Classification

The successful use of the 2005 high-resolution Quickbird classification to map historical land cover patterns in the 1990 Landsat image was largely due to the successful identification of changed areas and the use of boosted CT. NDVI image differencing's ability to identify change is a testament to the method's robustness in capturing vegetation loss and tolerance of topographic variables. The speckled mountain slope indicates that some false positive change could have been identified. These changes could be related to

difference in vegetation health, abundance, or structure between years, annual variation in snow melt, and/or residual geometric errors.

NDVI differencing did not capture all differences between dates. The two images used represent snapshots of the land's surface at two moments in time. Forest areas that could have been clear cut prior to 1990 and in the phase of regrowth in 1990 and in 2005 were not captured by the NDVI differencing method. This might be a deficiency of the NDVI differencing method for vegetation monitoring purposes. Our study, however, was not about forest management practices or vegetation dynamics. The appropriate method of change identification is therefore related to the change one seeks to identify, and NDVI differencing worked well for identifying MRD.

The success in the change identification resulted in the successful classification of the 1990 Landsat image. The classification was largely based on the assumption that areas with minimal change in NDVI were really areas of no change. A current classification with a known accuracy and known land cover could then be used to map the historical image. Taking the classified changed areas and merging them with the current classification reduced the compound error often associated with multiple classifications (Howarth and Wickware, 1981). Compound error arises in independent classifications because sources of error in the two classifications are largely independent. Compound error can reduce the accuracy of the post classification comparison methods by multiplying the error rates in each classification and greatly reducing the accuracy of the comparison. Compound error is reduced in the approach used in this study by classifying a large portion of the study area, which did not change between the two dates, only once.

Analysis of Temporal Change

Impervious surfaces encapsulated many different types of spectrally similar LULC types in both classifications. Impervious surfaces represented the scree and talus present on the mountain peaks and slopes, while at the same time representing human induced land cover such as roads and residential and commercial development. The amalgamated land cover that impervious surfaces represented was of limited utility for the individual classifications, but did provide great insight into our temporal analysis because change from vegetated to impervious surface was likely associated with increased MRD.

The 2005 classification had 1184.6 ha more area classified as impervious surfaces than in the 1990 classification. This cannot be related to absolute increases in impervious surfaces because the 30-m pixel size resulted in an abundance of pixels with mixed classes and pixels were classified as impervious if 20% of the pixel contained impervious surfaces. The 20% threshold was chosen in order to capture all impervious surfaces including small narrow roads, which could have otherwise been excluded. The increase in impervious surface was mirrored by a 944 ha decrease in forest and a 269.6 ha decrease in grasslands. No catastrophic natural events occurred between the two dates that could have caused such an increase. Forests and grasslands/shrublands conversion to impervious surfaces were therefore likely a result of MRD induced land cover changes.

Results from the descriptive statistics indicated the conversion of forests and grasslands to impervious surfaces was not proportional to their respective land cover in 1990. This is evident in the 67% of change being forest when forest only accounted for 51% of the land cover in 1990. This significant amount of forest loss can have negative

repercussions for ecosystems within the area. Most of the forest loss has a linear spatial pattern. This is likely a result of the addition of ski runs to the landscape. These linear patches differ from forest logging patches such as clear cuts in that the linear patches create multiple smaller patches of forest. This results in more habitat fragmentation than would have occurred with a clear cut. The effects of habitat fragmentation have been shown to result in decreases in species composition, distribution, and abundance for both flora and fauna (Odell et al., 2003; Crooks, 2002; Miller et al., 1998).

Previous studies have found topographic variables useful for identifying amenity development (Cromartie and Wardell, 1999). Our topographic variables, aspect and slope, did not provide much information on the proportion of change between 1990-2005 to land cover in 1990. They did explain some of the variance in the CT model. Aspect was used in the CT to separate two small groups of FI and FG. Slope was used to separate four different groups of change in the CT.

The indicator variables, distance-to-streams and distance-to-roads, were effective at explaining some of the variance within our change data. Forest and grassland changes, in general, were found closer to roads than they were found in 1990. This, however, was at least in part a result of roads being the actual change identified. MRD also generally includes road development for access. Previous studies have found that the introduction of roads to the landscape often facilitates development (Price, 2002). Accurate road data, however, does not exist for 1990. We cannot, therefore, determine if this is true for our case. We can use today's roads, however, to identify possible area of future development.

The variable distance-to-stream provided good information on our types of change. Previous studies have found that proximity of water is a good indicator of amenity development (Parmenter et al., 2003; Cromartie and Wardell, 1999). Our data showed that development of grasslands was disproportionately closer to streams than grasslands in general. This could likely be a result of amenity development at or near the water edges (Williams and McMillan, 1983; Williams and Jobes, 1990). The proximity of Meadow Village, a major focus of development, to the West Fork of the Gallatin River, certainly accounts for a large portion of this change. Forest change, however, was found farther away than the mean forest land in 1990. These relationships could also be a result of grasslands naturally occurring closer to water on average than forested land, which often occurs on upland mountain slopes.

Conclusion

High-resolution imagery was successfully merged with moderate-resolution imagery to map changes in land cover patterns in Big Sky, Montana. Previous research in this area has been lacking. Our research indicated that the generalization of a high-resolution classification can be used as training data for a historical image. This approach shows promise as a method of temporally monitoring LULC changes.

The use of NDVI image differencing and boosted CT resulted in the successful identification of land use change due to MRD. The NDVI differencing method allowed only areas of change to be identified and reclassified. This decreased the compound error often associated with post classification comparisons. Boosted CT handled both the

Landsat data and derived vegetation indices well. This is largely a result of the robustness of the classifier. Future research should include mapping more than two dates. This can allow for more information on the rate and nature of changes between years.

Statistical pattern analysis demonstrated that our indicators could be used to explain the change within our study area. We found forest changes to have a disproportionate amount of change when compared to the overall amount of forested area in 1990. We also found that forest changes were located farther away from streams and tended to occur on lower slopes. Grassland change tended to occur closer to streams. Overall changes in grasslands was proportional to the 1990 amount of land cover. These indicator variables explained 87% of the variance for the change classes and might be related to amenity development.

CHAPTER 5

CONCLUSION

Mountain Resort Development (MRD) is rapidly changing the landscape of the intermountain west. The emerging pattern is a shift from a primary extractive economy to a tertiary economy. The result of MRD is changes in LULC, which can affect ecosystems within the developed area, adjoining undeveloped areas, and downstream and riparian systems. Big Sky, Montana, provided a valuable opportunity to assess current and historical LULC patterns associated with MRD. Current LULC patterns in Big Sky were identified by creating a detailed classification using high-resolution imagery (multispectral and LiDAR) with object-oriented analysis. Historical land cover patterns were analyzed using change detection methods and descriptive statistical methods.

Results of this study indicated object-oriented analysis and classification was an effective means of creating detailed LULC maps with high-resolution imagery. Object-oriented classification has the ability to overcome the spectral limitations of high-resolution sensors through the addition of contextual metrics to the classification process. This creates additional dimensions for separating spectrally similar classes. The classified LULC maps in this study based on Quickbird imagery had an overall accuracy of 90% for both levels of the classification hierarchy. This exceeded USGS standards for remotely sensed classifications.

Image fusion in the form of combined multispectral information and elevation information derived from LiDAR first and last returns created more realistic objects than

multispectral objects alone. Object-oriented classification of a fused Quickbird and LiDAR image resulted in reduced error rates for individual classes compared to the Quickbird classification. The two classifications were not, however, statistically different. The overall accuracy for the fused image was 91% for both levels of the classification hierarchy. The fused classification resulted in a visually appealing classification with objects that better resembled their real world land cover classes. This was a result of a finer segmentation produced by the addition of the LiDAR data to the classification.

Future research opportunities for object-oriented classification and analysis are numerous. The identification of the appropriate spatial resolution for use with object-oriented classification is essential. This might prevent the creation of mixed land cover objects caused by the pixilated effect seen with the Quickbird imagery. Research into the full utilization of contextual metrics offered by the object-oriented software is also recommended. Object-oriented software also needs to be programmed to enable efficient handling of large images so as to make full use of the today's high resolution data.

Temporal analysis of land cover patterns was accomplished by successfully using a generalized version of the high-resolution land cover map as baseline data combined with NDVI image differencing based on Landsat imagery. This essentially resulted in the calibration of the historical Landsat image based on the Quickbird and LiDAR object-oriented classification. Previous research on multitemporal mapping of multiresolution images has been lacking. Our research indicated that the generalization of a high-

resolution classification can be used as training data for a historical image. This shows promise as a method of temporally monitoring LULC changes.

NDVI image differencing and boosted classification trees resulted in the successful identification of temporal changes in land cover due to MRD. The NDVI differencing method successfully identified the land cover change due to vegetation loss and was not affected by the topography of the study area. This allowed for the identification and classification of change areas only. The classified change areas were then merged with the unchanged current land cover classification. The merging process effectively decreased the compound error associated with multiple classifications.

Numerous future research possibilities exist for multitemporal mapping of multiresolution images. Mapping more than two dates is recommended. This can allow for more information on the rate and nature of changes between years to be gleaned. The land cover classes used for temporal analysis in our study were broad and general. An attempt should be made to identify how fine a classification can be generated from the high resolution classification.

Statistical pattern analysis demonstrated that distance-to-streams, distance-to-roads, slope, and aspect were all correlated to change within our study area. Forest changes were found to be disproportionate to their landscape amounts in 1990. Forest changes were also found to be located farther away from streams and on lower slopes than their 1990 proportions. Grassland change tended to occur closer to streams. Overall changes in grasslands, however, were proportional to their 1990 land cover. These variables explained 87% of the variance for the change classes and might be related to amenity development.

The statistical pattern analysis also indicated an increase in impervious surfaces between the years 1990-2005. This increase in impervious surface resulted in a decrease in both forests and grassland areas. Loss of forest and grassland area increases habitat fragmentation and can have negative consequences for ecosystems within the area.

LITERATURE CITED

- Allen, T. R., and Kupfer, J. A., 2000. Application of spherical statistics to change vector analysis of Landsat data southern Appalachian spruce-fir forests. *Remote Sensing of Environment* 74:482-493.
- Baker, C., Lawrence, R., Montagne, C., and Patten, D., 2007. Change detection of wetland and riparian ecosystems using change vector analysis. *Wetlands* 27:610-619.
- Baker, C., Lawrence, R., Montagne, C., and Patten, D., 2006. Mapping wetlands and riparian areas using Landsat ETM+ imagery and decision tree-based models. *Wetlands* 26:465-474.
- Baron, J. S., Theobald, D. M., and Fagre, D. B., 2000. Management of land use conflicts in the United States Rocky Mountains. *Mountain Research and Development* 20:24-27.
- Benz, U. C., Hofmann, P., Willhauck, G., Lingenfelder, I., and Heynen, M., 2004. Multi-resolution, object-oriented fuzzy analysis of remote sensing data for GIS-ready information. *ISPRS Journal of Photogrammetry and Remote Sensing* 58:239-256.
- Bricklemyer, R.S., Lawrence, R.L., Miller, P.R., and Battogtokh, N., 2007. Monitoring and verifying agricultural practices related to soil carbon sequestration. *Agriculture, Ecosystems and Environment* 118:201-210.
- Brown, K., Turner, R. K., Hameed, H., and Bateman, I., 1997. Environmental carrying capacity and tourism development in the Maldives and Nepal. *Environmental Conservation* 24:316-325.
- Budreski, K. A., Wynne, R. H., Browder, J. O., and Campbell, J. B., 2007. Comparison of segment and pixel-based non-parametric land cover classification in the Brazilian Amazon using multitemporal Landsat TM/ETM+ imagery. *Photogrammetric Engineering and Remote Sensing* 73:813-827.
- Carleer, A. P., and Wolff, E., 2006. Urban land cover multi-level region-based classification of VHR data by selecting relevant features. *International Journal of Remote Sensing* 27:1035-1051.
- Carrao, H., Caetano, M., and Coelho, P. S., 2007. Sample design and analysis for thematic map accuracy assessment: An approach based on domain estimation for the validation of land cover products. *Proceedings of 32nd International Symposium on Remote Sensing of Environment, Costa Rica* June 25-29, 2007.

- Chubey, M. S., Franklin, S. E., and Wulder, M. A., 2006. Object-based analysis of Ikonos-2 imagery for extraction of forest inventory parameters. *Photogrammetric Engineering & Remote Sensing* 72:383-394.
- Collins, J. B., and Woodcock, C. E., 1996. An assessment of several linear change detection techniques for mapping forest mortality using multitemporal Landsat TM data. *Remote Sensing of Environment* 1: 66-77.
- Congalton R. C., and Green, K., 1999. *Assessing the accuracy of remotely sensed data: Principles and Practices*. Lewis Publishers, New York.
- Coppin, P., Jonckheere, I., Nackaerts, K., and Muys, B., 2004. Digital change detection methods in ecosystem monitoring: A review. *International Journal of Remote Sensing* 19:411-426.
- Crist, E. P., and Cicone, R. C., 1984. A physically-based transformation of Thematic Mapper data the TM tasseled cap. *IEEE Transactions of Geosciences and Remote Sensing* 25:1565-1596.
- Cromartie J. B., and Wardwell J. M., 1999. Migrants settling far and wide in the rural West. *Rural Development Perspectives* 14:2-8.
- Crooks, K. R., 2002. Relative Sensitivities of Mammalian Carnivores to Habitat Fragmentation. *Conservation Biology* 16:488-502.
- De'ath, G., and Fabricius, K. E., 2002. Classification and Regression Trees: A powerful yet simple technique for ecological data analysis. *Ecology* 81:3178-3192.
- Definiens Professional 5: LDH, 2007. User's Guide.
- Definiens Professional 5: LDH, 2007. Reference Manual.
- Friedl, M. A., and Brodley, C. E., 1997. Decision tree classification of land cover from remotely sensed data. *Remote Sensing of Environment* 61:399-409.
- Gardener, K. K., and Vogel, R. M., 2005. Predicting groundwater nitrate concentrations from land use. *Groundwater* 43:343-352.
- Green, K., and Lopez, C., 2007. Using Object-Oriented Classification of ADS40 to map benthic habitats of the state of Texas. *Photogrammetric Engineering and Remote Sensing* 73:861-865.

- Groffman, P. M., Bain, D. J., Band, L. E., Belt, K. T., Brush, G. S., Grove, J. M., Pouyat, R. V., Yesilonis, I. C., Zipperer, W. C., 2003. Down by the riverside: Urban riparian ecology. *Frontier in Ecology and the Environment*. 6:315-321.
- Guerra, F., Puig, H., and Chaume, R., 1998. The forest-savanna dynamics from multi-date Landsat TM in Sierra Parima, Venezuela. *International Journal of Remote Sensing* 19:2061- 2075.
- Haala, N., and Brenner, C., 1999. Extraction of buildings and trees in urban environments. *ISPRS Journal of Photogrammetry & Remote Sensing* 54:130-137.
- Hansen, A. J., Rasker, R., Maxwell, B., Rotella, J. J., Johnson, J. D., Wright Parmenter, A., Langer, U., Cohen, W. B., Lawrence, R. L., and Kraska, M. P.V., 2002. Ecological causes and consequences of demographic change in the New West. *Bioscience* 52:151-162.
- Herold, M., Gardner, M. E., and Roberts, D. A., 2003. Spectral resolution requirements for mapping urban areas. *IEEE Transactions on Geoscience and Remote Sensing* 41:1907-1919.
- Herold, M., Roberts, D. A., Gardner, M. E., and Dennison, P. E., 2004. Spectrometry for urban area remote sensing—development and analysis of a spectral library from 350 to 2400 nm. *Remote Sensing of Environment* 91:304-319.
- Herold, M., and Scepan, J., Muller, A., and Gunther, S., 2002. Object-oriented mapping and analysis of urban land use/cover using IKONOS data. *Proceedings of 22nd EARSEL Symposium for European-wide integration, Prague*.
- Herold, M., Gardner, M. E., and Roberts, D. A., 2003. Spectral resolution requirements for mapping urban areas. *IEEE Transactions on Geoscience and Remote Sensing* 41:1907-1919.
- Hill, R. A., and Thomson, A. G., 2005. Mapping woodland species composition and structure using airborne spectral and LiDAR data. *International Journal of Remote Sensing* 26:3763-3779.
- Hyde, P., Dubaya, R., Walker, W., Blair, J. B., Holten, M., and Hunsaker, C., 2006. Mapping forest structure for wildlife habitat analysis using multi-sensor (LiDAR, SAR/InSAR, ETM+, Quickbird) Synergy. *Remote Sensing of Environment* 102:63-73.
- Howarth, P. J., and Wickware, G. M., 1981. Procedures for change detection using Landsat. *International Journal of Remote Sensing* 12:1471-1491.

- Johnson, R. D., and Kasischke, E. S., 1998. Change vector analysis: A technique for the multi-spectral monitoring of land cover and condition. *International Journal of Remote Sensing* 19:411-426.
- Kuehn, S., Benz, U., and Hurley, J., 2002. Efficient flood monitoring based on RADARSAT-1 images data and information fusion with object-oriented technology. *IEEE Transactions on Geoscience and Remote Sensing Symposium*.
- Laberte, A. S., Rango, A., Havstad, K. M., Paris, J. F., Beck, R. F., McNeely, R., and Gonzalez, A. L., 2004. Object-oriented image analysis for mapping shrub encroachment from 1937 to 2003 in Southern New Mexico. *Remote Sensing of Environment* 93:198-210.
- Lawrence, R., Bunn, A., Powell, S., Zambon, M., 2004. Classification of remotely sensed imagery using stochastic gradient boosting as a refinement of classification tree analysis. *Remote Sensing of Environment* 3:331-336.
- Li, X., and Yeh, A. G. O., 1998. Principal component analysis of stacked multi-temporal images for the monitoring of rapid urban expansion in the Pearl River Delta. *International Journal of Remote Sensing* 19:1501-1518.
- Liu, X., and Lathrop, R. G., 2002. Urban change detection based on an artificial neural network. *International Journal of Remote Sensing* 23:2513-2518.
- Lu, D., Mausel, P., Brondizio, E., and Moran, E., 2003. Change detection techniques. *International Journal of Remote Sensing* 25:2365-2407.
- Lynn, N. A., and Brown, R. D., 2003. Effects of recreational use impacts on hiking experiences in natural areas. *Landscape and Urban Planning* 64:77-87.
- Lyon, J. G., Yuan, D., Lunetta, R. S., Elvidge, C. D., 1998. A change detection experiment using vegetation indices. *Photogrammetric Engineering and Remote Sensing* 64:143-150.
- Marston, Richard A., and Anderson, J. E., 1991. Watersheds and vegetation of the Greater Yellowstone Ecosystem. *Conservation Biology* 5:338-346.
- Mas, J. F., 1999. Monitoring land-cover changes: A comparison of change detection techniques. *International Journal of Remote Sensing* 20:139-152.
- McCombs, J. W., Roberts, S. D., and Evans, D. L., 2003. Influence of fusing LiDAR and multi-spectral imagery on remotely sensed estimates of stand density and mean tree height in a managed loblolly pine plantation. *Forest Science* 49:457-466.

- Miller, S. G., Knight, R. L., and Miller, C. K., 1998. Influence of recreational trails on breeding bird communities. *Ecological Applications* 8:162-169.
- Mitri, G. H., and Gitas, I. Z., 2004. A performance evaluation of a burned area object-based classification model when applied to topographically and non-topographically corrected TM imagery. *International Journal of Remote Sensing* 25:2863-2870.
- Moeller, M., and Blaschke, T., 2006. A new index for the differentiation of vegetation fractions in urban neighborhoods based on satellite imagery. *ASPRS Annual Conference, Reno Nevada 2006*.
- Odell, E. A., Theobald, D. M., and Knight, R. L., 2003. Incorporating ecology into land use planning: The songbirds' case for clustered development. *Journal of American Planning and Association* 69:72-82.
- Parmenter Wright, A., Hansen, A., Kennedy, R. E., Cohen, W., Langner, U., Lawrence, R., Maxwell, B., Gallant, A., and Aspinall, R., 2003. Land use and land cover change in the Greater Yellowstone Ecosystem:1975-1995. *Ecological Applications* 13:687-703.
- Pohl, C., and Van Genderen, J. L., 1998. Multi-sensor image fusion in remote sensing: Concepts, methods and applications. *International Journal of Remote Sensing* 19:823-854.
- Price, M. F., 1992. Patterns of the development of tourism in mountain environments. *GeoJournal* 27:87-96.
- Reed, R. A., Johnson-Barnard, J., and Baker, W., 1996. Contributions of roads to forest fragmentation in the Rocky Mountains. *Conservation Biology* 10:1098-1106.
- Ridd, M. K., and Liu, J., 1998. A comparison of four algorithms for change detection in an urban environment. *Remote Sensing of Environment* 63:95-100.
- Riebsame, W. E., Gosnell, H., and Theobald, D. M., 1996. Land Use and Landscape change in the Colorado mountains 1: Theory, scale, pattern. *Mountain Research and Development* 16:395-405.
- Ries, J., 1996. Landscape damage by skiing at the Schauinsland in the Black Forest, Germany. *Mountain Research and Development* 16:27-40.
- Rouse, J. W., Haas, R. H., Schell, J. A., Deering, D. W., and Harlan, J. C., 1973. Monitoring the vernal advancement of retrogradation (green wave effect) of natural vegetation. *NASA/GSFC Type III Final Report, Greenbelt, MD*.

- RuleQuest Research, 2008. Data Mining Tools See5 and C5.0 2.05.
- Sauvajot, R. M., Buechner, M., and Kamradt, C. M., 1998. Patterns of human disturbance and response by small mammals and birds in chaparral near urban development. *Urban Ecosystems* 2:279-297.
- Sawaya, K. E., Olmanson, L. G., Heinert, N. J., Brezonik, P. L., and Baur, M. E., 2003. Extending satellite remote sensing to local scales: Land and water resource monitoring using high-resolution imagery. *Remote Sensing of Environment* 88:144-156.
- Shanley, J. S., and Wemple, B. C., 2002. Water quality and quantity in the mountain environment. *Vermont Law Review* 26 (3):717-751.
- Shiba, M., and Itaya, A., 2006. Using eCognition for improved forest management and monitoring systems in precision forestry. *Proceeding of the International Recision Forestry Symposium, Stellenbosch University*.
- Venables, W. N., and Ripley, B. D., 1997. *Modern Applied Statistic with S-plus Second Edition*, Springer-Verlas, New York, NY, 5489.
- Walker, J. S., and Briggs, J. M., 2007. An object-oriented approach to urban forest mapping in Phoenix. *Photogrammetric Engineering and Remote Sensing* 73:577-583.
- Wang, L., Sousa, W. P., and Gong, P., 2004. Integration of object-based and pixel-based classification for mapping mangroves with IKONOS imagery. *International Journal of Remote Sensing* 20:5655-5668.
- Weaver, J. L., Paquet, P. C., and Ruggiero, L. F., 1996. Resilience and conservation of large carnivores in the Rocky Mountains. *Conservation Biology* 10:964-976.
- Wemple, B. C., Jones, J. A., and Grant, G. E., 1996. Channel network extension by logging roads in two basins, Western Cascades, Oregon. *Water Resources Bulletin* 32:1195-1207.
- Wemple, B. C., Swanson, F. J., and Jones, J. A., 2001. Forested roads and geomorphic process interactions, Cascade Range, Oregon. *Earth Surface Processes and Landforms* 26:191-204.
- Williams, A. S., and McMillan, D. B., 1983. Location specific capital and destination selection among migrants to non-metro areas. *Rural Sociology* 48:457-497.

- Williams, A. S., and Jobes, P. C., 1990. Economic and quality of life considerations in urban-rural migration. *Journal of Rural Studies* 6:187-194.
- Yuan, F., and Bauer, M., 2006. Mapping impervious surface area using high resolution imagery A comparison of object-based and per pixel classification. *ASPRS Annual Conference* May 20